



A review of tunnel rockburst prediction methods based on static and dynamic indicators

Qinghe Zhang^{1,2} · Weiguo Li¹ · Liang Yuan² · Tianle Zheng¹ · Zhiwei Liang¹ · Xiaorui Wang¹

Received: 17 September 2023 / Accepted: 30 April 2024
© The Author(s), under exclusive licence to Springer Nature B.V. 2024

Abstract

Rockbursts frequently occur in tunneling projects and pose a serious threat to workers and the environment. Therefore, accurate prediction of rockbursts is of great practical significance. Currently, various rockburst prediction methods exist, with static and dynamic indicators playing a key role. This paper analyzes the importance of rockburst prediction methods based on Citespace software. The results indicate that microseismic monitoring, acoustic emission, and machine learning are the most important methods. The paper focuses on four common rockburst prediction methods: empirical methods, microseismic monitoring, acoustic emission, and machine learning, from the perspective of static and dynamic indicators. The performance and application of static and dynamic indicators in the four common prediction methods in recent years are summarized, the limitations of static and dynamic indicators at this stage are discussed, and possible future development directions are proposed. This paper provides the necessary perspective and tools for better understanding the advantages and disadvantages of static and dynamic indicators in the four rockburst prediction methods.

Keywords Rockburst · Rockburst prediction methods · Static indicators · Dynamic indicators · Citespace software

List of symbols

σ_{θ}	Tangential stress in surrounding rock, MPa
σ_c	Uniaxial compressive strength of rock mass, MPa
R_b	Uniaxial saturated compressive strength
NDS	Normalized bias stress
σ_1	Maximum principal in situ stress, MPa
R_t	Uniaxial tensile strength
B_i	Rock brittleness coefficient, σ_c/σ_t

✉ Qinghe Zhang
zhangqhsdu@163.com

¹ School of Civil Engineering and Architecture, Anhui University of Science and Technology, Huainan 232001, China

² State Key Laboratory Mine Response and Disaster Prevention and Control in Deep Coal Mine, Anhui University of Science and Technology, Huainan 232001, China

BIM	Brittleness index modified
BSR	Brittle shear ratio
W_{TG}	Rockburst index
M_{coal}	Modulus after destruction
E	Young's modulus, GPa
K _{cr}	Critical mining stress index
K_v	Rock mass integrity coefficient
S	Stress index
W_{et}	Strain energy storage index, kJ m^{-3}
I_{RB}	Rockburst risk index
H	Buried depth in the tunnel, m
σ_{RB}	Maximum stress of rockburst, MPa
R_0	Tunnel diameter
σ'_3	Minimum principal stress at destruction, MPa
σ_t	Tensile strength of rock mass, MPa
A'_{CF}	Peak energy impact index
σ_0	Maximum ground stress in the surrounding rock before excavation
ε_p	Peak strain
$LERS_i$	Localized energy release rate
U_h	The energy dissipated to overcome frictional and support resistance during impact ground pressure, kJ m^{-3}
RPI	Rockburst propensity index
σ'_{rm}	Triaxial rock strength based on the Hoek–Brown strength criterion
DT	Failure duration index
U_{ET}^e	Elastic strain energy density at the unloading level
U_{ET}^d	Dissipated energy density at the unloading level
W_P	Energy conservation index
W_E	Work done by pressure
ε_r	Residual strain
ω_e	Pre-peak elastic energy density
φ_{st}	Dissipative strain energy
B_q	Rockburst energy index
U_e^e	Elastic strain energy density
U_d^d	Destructive energy density
RERI	Relative energy release index
LERR	Local energy release rate
U_{imin}	Minimum elastic strain energy density
U_e	Elastic energy density at peak
U_{BIM}^0	Peak elastic strain energy density
U_d	Dissipated energy density at peak
φ_{sp}	Elastic strain energy
σ_p	Peak stress
W_{ET}^p	Peak strength strain energy storage index
σ_r	Residual stress
K_{ED}^p	The ratio of peak point elastic strain energy to dissipation energy
E_{imax}	Maximum strain energy density
E_{imin}	Minimum strain energy density
K_{ED}^j	The ratio of elastic strain energy to dissipation energy at the failure point

1 Introduction

With the continuous development of tunneling to large depths and high-stress directions, rockburst disasters began to appear frequently. Rockburst is a kind of excavation process in the rock mass of the energy stored in the sudden release, resulting in rock burst, spalling, ejection, and other phenomena of geological hazards, with a strong suddenness, randomness, and harm (Li et al. 2019; Liang et al. 2020c; Du et al. 2022). The earliest recorded rockburst incident took place in England at the Leipzig Coal Mine (Kaiser et al. 1996). Subsequently, rockburst of varying magnitudes has occurred in tunnels, shafts, caves, and mines worldwide (Wang et al. 2018b, 2019; Tao et al. 2019). Rockbursts have occurred in China's Qinling Tunnel (Wang et al. 2023b), Yuyangshan Tunnel (Wu et al. 2021), the Hanjiang River to Weihe River diversion tunnel (Liu et al. 2019), the Jinping II Hydroelectric Power Station diversion tunnel (Gong et al. 2012), as well as Canada's Cigar Lake Uranium Mine (Morgenroth et al. 2022), resulting in significant economic losses and casualties. Today, achieving precise rockburst prediction remains a significant challenge. Therefore, how to accurately and efficiently make predictions about rockbursts has become one of the many research hotspots.

Studies have shown that whether or not a rockburst occurs depends on the stability of the rock mass, which depends on the mechanical properties of the rock (e.g. strength, stiffness, and modulus of elasticity, etc.) and external conditions (e.g. dynamic disturbance, magnitude of in situ stresses and geological structure, etc.) (Liu et al. 2013; Meng et al. 2017). Currently, scholars have established a large number of static parameters based on factors such as rock mechanical properties and strain energy evolution, including the rock mass integrity coefficient K_v , buried depth in the tunnel H , maximum ground stress in the surrounding rock before excavation σ_0 , maximum tangential stress σ_θ , etc. Consequently, empirical index guidelines, exemplified by the Turchaninov criterion (Turchaninov et al. 1972), Barton criterion (Barton et al. 1974), Roussens criterion (Russenes 1974), Hoek and Brown criterion (Hoek and Brown 1997), Tao criterion (Tao 1988), strain energy storage index W_{et} (Kidybiński 1981), peak intensity strain energy storage index W_{et}^p (Gong et al. 2019), residual elasticity energy index C_{ef} (Gong et al. 2021) and five-factor criterion (Zhang et al. 2011) have been formulated as rockburst prediction criteria. In the construction stage, with the geological structure and rock stress state and other related static data gradually determined, the accuracy of trend prediction of rockburst disasters through the use of empirical methods has been significantly improved. However, for the higher risk of strong rockburst or very strong rockburst, the trend prediction of rockburst using empirical methods may have a lag phenomenon. The empirical method is mainly through indoor testing to obtain static parameters of rock samples, which can not reflect the real situation of the rock mass. It can not meet the requirements of real-time dynamic early warning at the construction site (He et al. 2021).

The emergence of surveillance systems and monitoring equipment has gradually transformed indicators from static to dynamic, making real-time dynamic early warning possible (Du et al. 2021). By monitoring the dynamic signals generated before and after rock ruptures, such as strain energy, elastic waves, electromagnetic radiation, and rock surface temperature, a diverse set of dynamic indicators has been established. These indicators encompass apparent stress, apparent volume, microseismic energy density, acoustic emission energy, ringer counts, electromagnetic radiation pulse counts, and infrared temperature jump rates (Wang et al. 2011; Dou et al. 2018; Ding et al. 2022; Hao et al. 2022). Consequently, A range of rockburst field monitoring techniques, including microseismic

monitoring method (Tang et al. 2021), acoustic emission method (Becker et al. 2010), electromagnetic radiation method (Rabinovitch et al. 2002), infrared thermal imaging method (Liu et al. 2023b), micro-gravity method (Adoko et al. 2013) and drilling cutting method (Zhou et al. 2012), etc., has been developed based on these dynamic indicators. Empirical methods and on-site monitoring methods have avoided casualties and economic losses to a certain extent. However, static and dynamic indicators are more difficult to obtain, and there are outstanding problems such as data outliers and difficulties in data processing. Thus limiting the predictive accuracy of empirical methods and field monitoring methods. Rockburst is the result of the combined effect of a variety of influencing factors, and the high degree of non-linear relationship between the factors so that empirical methods and field monitoring methods are difficult to realize the integrated prediction of multiple indicators, to a certain extent, reducing the prediction efficiency (Ma et al. 2018).

Advances in science and technology, as well as algorithmic modeling, have led to an extension of the application fields for machine learning approaches in recent years. Several academics have been devoted to the investigation of machine learning methods since Feng and Wang (1994) deployed neural network learning and adaptive recognition approaches for rockburst prediction. Four static indicators—rockburst ground stress, uniaxial compressive strength of rock mass, uniaxial tensile strength, and strain energy storage index—were employed by Dong et al. (2013) as input data for the random forest algorithm model for predicting rockbursts. Meanwhile, Ghasemi et al. (2019) used four static metrics, namely Stress coefficient, rock brittleness coefficient, strain energy storage index, and maximum tangential stress, as input data for the C5.0 decision tree algorithm, which explicitly showed the relationship between inputs and outputs. Dealing with non-linear relationships, high dimensionality, and small sample database problems is characteristic of the support vector machine algorithm model (Zhao et al. 2007). Zhou et al. (2023) used six dynamic metrics, namely angular frequency ratio, p-wave to s-wave energy ratio, cumulative micro-seismic energy, apparent stress, radius of concavity, and seismic moments, as input data to the support vector machine to perform rockburst prediction. Machine learning approaches have been shown in studies to be effective in dealing with static and dynamic index data, as well as non-linear connections between indicators, offering a vital tool for complete multi-indicator forecasting (Zhou et al. 2023).

Currently, rockburst prediction methods based on static and dynamic indicators are shown in Fig. 1. They mainly include empirical methods (Zhao et al. 2017; Gong et al. 2018a), experimental tests (Cai 2016), numerical modeling (Xue et al. 2021), machine learning method (Shirani Faradonbeh et al. 2020; Li et al. 2023c) and geophysical method (Feng et al. 2015; Meng et al. 2016; Wang et al. 2021a). Geophysical methods also include the microseismic monitoring method, acoustic emission method, hydraulic support pressure method, electromagnetic radiation method, infrared radiation method, microgravity method, and drill chip method. These methods can be categorized into two types: short-term prediction and long-term prediction (Pu et al. 2019a). Short-term rockburst prediction mainly refers to on-site monitoring of a localized area, such as microseismic monitoring and electromagnetic radiation, etc., with a shorter test cycle. Long-term prediction is a comprehensive assessment of the rockburst potential and site conditions, such as based on the mechanical properties of the rock and site conditions proposed by a variety of indicators of the method. Because it has a more intuitive appearance and is widely used in the field of rockburst prediction (Zhou et al. 2018a; Afraei et al. 2019). However, there is no article to systematically summarize the rockburst prediction methods from the perspective of static and dynamic indicators. Therefore, it is necessary to analyze the application of static and dynamic indicators in rockburst prediction methods.

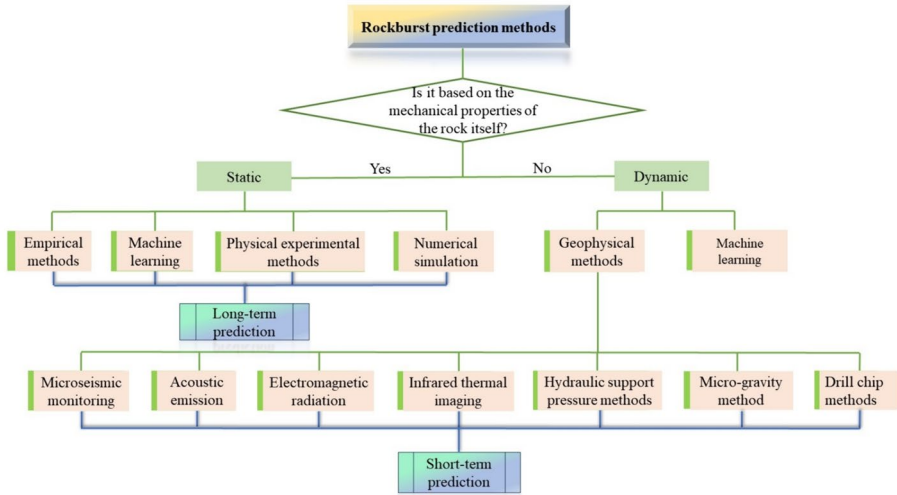


Fig. 1 Schematic diagram of rockburst prediction methods

Based on the numerous rockburst prediction methods demonstrated in Fig. 1, this paper aims to analyze four rockburst prediction methods, namely empirical methods, microseismic monitoring, acoustic emission, and machine learning, which are commonly used nowadays, from the perspectives of static and dynamic indicators. First, the importance of various rockburst prediction methods is analyzed based on Citespace software. Then, the application of static and dynamic indicators in the four rockburst prediction methods is analyzed. Finally, the advantages and disadvantages of static and dynamic indicators in rockburst prediction methods and their problems are discussed. The possible future development direction is proposed to provide a useful reference for the rockburst prediction research.

2 Analysis of the importance of rockburst prediction methods

The topic of rockburst prediction is exceedingly complicated, and no mature and full theory and technology exists. Since the beginning of the rockburst disaster, numerous scholars have created a series of study outcomes based on static and dynamic indicators of rockburst prediction research. A scientometric analysis of rockburst prediction methods is required to better grasp the existing area of knowledge and investigate the value of various rockburst prediction methods.

Citespace, as one of the scientometric analysis software, has the advantage of tracking the research frontiers (Liang et al. 2020a). In this chapter, Citespace software is used to visualize and analyze the rockburst prediction methods.

The keyword co-occurrence network is shown in Fig. 2. The size of the keyword in the figure reflects the frequency of that keyword, i.e., the larger the keyword, the more frequently it appears. The blue bar graph in Fig. 3 reflects the specific frequency size of the keyword. From Figs. 2 and 3, it can be found that mechanism, energy, stress, numerical simulation, model, and classification are the keywords with a relatively high frequency of occurrence. Among them, mechanisms appeared 68 times, and energy and

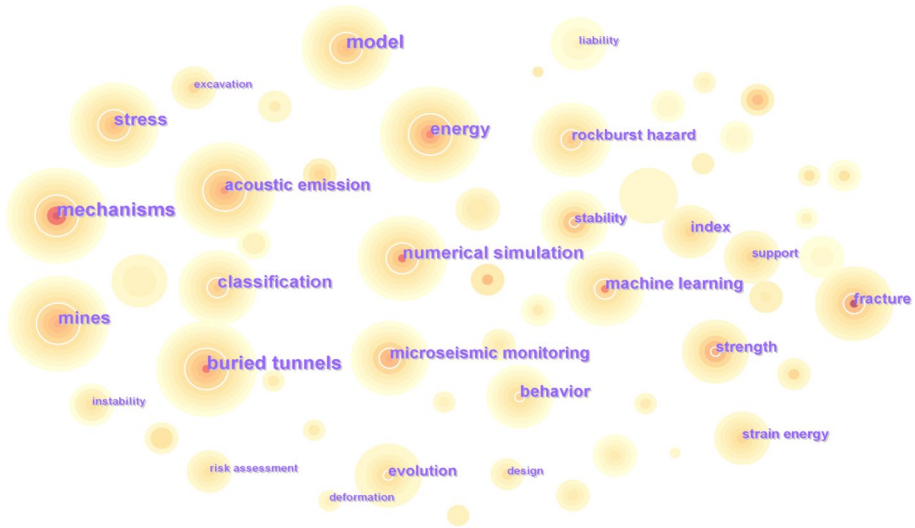


Fig. 2 Keyword co-occurrence map for rockburst prediction for the period 2007–2023

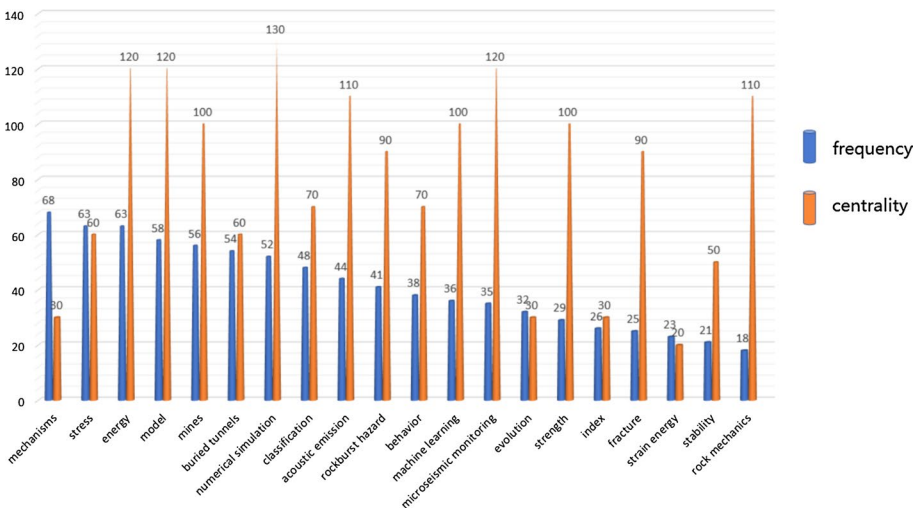


Fig. 3 Frequency of occurrence of the first 20 keywords and their centrality

stress appeared 63 times. It indicates that the study of the evolution of energy and stress in the process of rock damage using model tests and numerical analysis is the main way to understand the mechanism of rockburst occurrence (Zhao et al. 2021; Cui and Wong 2023; Su et al. 2023). At the same time, it shows that the rockburst mechanism is closely integrated with rockburst prediction. The ultimate goal of understanding the rockburst mechanism is to accurately predict rockburst hazards, and rockburst prediction can be implemented more effectively by exploring the rockburst mechanism.

Acoustic emission, machine learning, and microseismic monitoring appear frequently, indicating that the research for rockburst prediction mainly focuses on the three methods of acoustic emission, machine learning, and microseismic monitoring. Centrality refers to the mediating role played by a keyword in the transmission of information, reflecting the academic importance of that keyword (Fu et al. 2022). Figure 2 shows the centrality of the top 20 keywords. The orange bars reflect the magnitude of the centrality of the keywords. (The values in the graph are actual centrality $\times 10^3$). The results show generally high centrality of acoustic emission, machine learning, and microseismic monitoring. It indicates a crucial transfer value in the field of rockburst prediction. For example, microseismic monitoring can be directly used for field prediction, while the dynamic data it generates can be used as input data for machine learning methods, furthermore, microseismic monitoring has a similar working principle to acoustic emission. There are many other cases where a keyword radiates to two or more keywords, and the centrality can be used to understand the range and intensity of a keyword's radiation. The number of occurrences of index in the figure is low and the centrality is not high. It shows that the use of various indicators for direct rockburst prediction is relatively less used, such as empirical methods.

3 Rockburst prediction methods based on static indicators

In the case of the rockburst mechanism has not been studied clearly (Liu et al. 2022), scholars have established a large number of static indicators based on engineering experience and rockburst influence factors. It is also known as the empirical method of rockburst prediction, which is widely used in practical engineering. At present, the empirical methods are mainly divided into empirical methods with single indicators and empirical methods with multi-index indicators (Wu et al. 2019).

3.1 Empirical methods with a single indicator

For the prediction problem of rockburst susceptibility, a large number of single evaluation indicators have been established from the perspective of a series of theories such as strength, energy, deformation, and stiffness. Among them, the majority of judgment indicators are in terms of stress and energy (Liu et al. 2013; Zhou et al. 2018a; He et al. 2021). This section summarises the empirical methods developed based on static indicators from the energy and stress perspectives.

3.1.1 Stress methods

The stress method has a variety of physical metrics that characterize the rock features. These include key factors such as the geometrical and mechanical parameters of the intact rock, the pathological stresses, and the magnitude of the induced stresses. Evaluation indicators based on these factors have been validated for rockburst prediction (Gong and Li 2007). Table 1 summarises the empirical methods based on strength theory that have emerged in recent years, along with their associated judgments and rockburst classification. However, there is no generalized rockburst criterion that can fully encompass all practical engineering conditions. Previously, a large number of criterion guidelines have been proposed based on the σ_1/σ_c , $\sigma_{\theta,\max}/\sigma_c$ and $(\sigma_{\theta} + \sigma_l)/\sigma_c$ indices, such as Barton's criterion, Tao's criterion, Hoek and Brown's criterion, Russenes' criterion and Turchaninov's

Table 1 Summary of rockburst criteria based on strength theory and assessment of qualitative indicators for rockburst grading

Serial number	References	Index and/or equations	Intensity grading
1	Hosseini et al. (2010)	$NDS = (\sigma_1 - \sigma_3) / \sigma_c$	<p>$NDS < 0.35$ None rockburst</p> <p>$0.35 \leq NDS < 0.50$ Light rockburst</p> <p>$0.50 \leq NDS < 0.80$ Medium rockburst</p> <p>$0.80 \leq NDS \leq 1.00$ Heavy rockburst</p> <p>$NDS > 1.00$ Serious rockburst</p>
2	Zhang et al. (2011)	$B_3 = \sigma_c / \sigma_t$	<p>$B_3 < 15.00$ None rockburst</p> <p>$15.00 \leq B_3 < 18.00$ Light rockburst</p> <p>$18.00 \leq B_3 \leq 22.00$ Medium rockburst</p> <p>$B_3 > 22.00$ Heavy rockburst</p>
3	Castro et al. (2012)	$BSR = (\sigma_1 - \sigma_3) / \sigma_c$	<p>$0.35 \leq BSR < 0.45$ None rockburst</p> <p>$0.45 \leq BSR < 0.60$ Light rockburst</p> <p>$0.60 \leq BSR < 0.70$ Medium rockburst</p> <p>$BSR \geq 0.7$ Heavy rockburst</p>
4	Bukowska (2012)	$W_{TG} = M_{coal} / E_{rock}$	<p>$W_{TG} < 1.00$ None rockburst</p> <p>$1.00 \leq W_{TG} < 2.00$ propensity for rockbursts</p> <p>$W_{TG} > 2.00$ low tendency to rockburst</p>
5	Shang et al. (2013)	$P_{rb} = K \nu \sigma_0 / \sigma_t$	<p>$P_{rb} < 1.70$ None rockburst</p> <p>$1.70 \leq P_{rb} < 3.30$ Light rockburst</p> <p>$3.30 \leq P_{rb} < 9.70$ Medium rockburst</p> <p>$P_{rb} \geq 9.70$ Heavy rockburst</p>
6	Zhang et al. (2013)	$S = \tanh \left\{ \left[0.1648 \left(\frac{\sigma_0}{\sigma_c} \right)^{3.064} (B_3)^{-0.4625} (W_{at})^{2.672} \right]^{(1/3.6)} \right\}$	<p>$S < 0.25$ None rockburst</p> <p>$0.25 \leq S < 0.50$ Light rockburst</p> <p>$0.50 \leq S < 0.75$ Medium rockburst</p> <p>$S \geq 0.75$ Heavy rockburst</p>

Table 1 (continued)

Serial number	References	Index and/or equations	Intensity grading
7	He et al. (2015)	$I_{RB} = H/\sigma_{RB}$	$I_{RB} < 0.60$ Light rockburst $0.60 \leq I_{RB} < 1.20$ Medium rockburst $1.20 \leq I_{RB} < 2.00$ Heavy rockburst $I_{RB} \geq 2.0$ Serious rockburst
8	Zhang et al. (2016)	$\Omega = (3 - \lambda_0) W_{et} \sigma_\theta / \sigma_c$	$\Omega < 0.40$ None rockburst $0.40 \leq \Omega < 1.05$ Light rockburst $1.05 \leq \Omega < 2.50$ Medium rockburst $\Omega \geq 2.50$ Heavy rockburst
9	Zhao et al. (2017)	σ_c / σ_1	$\sigma_c / \sigma_1 > 5.00$ None rockburst $5.00 \geq \sigma_c / \sigma_1 > 4.00$ Light rockburst $4.00 \geq \sigma_c / \sigma_1 > 2.50$ Medium rockburst $2.50 \geq \sigma_c / \sigma_1 > 1.50$ Heavy rockburst $\sigma_c / \sigma_1 \leq 1.50$ Serious rockburst
		σ_θ / σ_c	$\sigma_\theta / \sigma_c \leq 0.20$ None rockburst $0.20 \leq \sigma_\theta / \sigma_c < 0.50$ Light rockburst $0.50 \leq \sigma_\theta / \sigma_c < 0.70$ Medium rockburst $0.70 \leq \sigma_\theta / \sigma_c < 0.90$ Heavy rockburst $\sigma_\theta / \sigma_c \geq 0.90$ Serious rockburst
		σ_c / σ_v	$\sigma_c / \sigma_v > 10.00$ None rockburst $10.00 \geq \sigma_c / \sigma_v > 5.00$ Light rockburst $5.00 \geq \sigma_c / \sigma_v > 3.30$ Medium rockburst $3.30 \geq \sigma_c / \sigma_v > 2.50$ Heavy rockburst $\sigma_c / \sigma_v \leq 2.50$ Serious rockburst

Table 1 (continued)

Serial number	References	Index and/or equations	Intensity grading
10	Ma et al. (2018)	$RPI = \sigma'_{Tm} / \sigma_{max} \sigma'_{Tm} = \sigma'_3 + \sigma_{ci} [m_b (\sigma'_3 / \sigma_{ci}) + s]^\alpha$	RPI > 7.00 None rockburst 7.00 ≥ RPI > 4.00 Light rockburst 4.00 ≥ RPI > 2.00 Medium rockburst 2.00 ≥ RPI > 1.00 Heavy rockburst RPI ≤ 1.00 Serious rockburst
11	Wang et al. (2018a)	B = R _b /R _t	B ≥ 40.00 None rockburst 40.00 > B ≥ 26.70 Light rockburst 26.70 > B ≥ 14.50 Medium rockburst B < 14.50 Heavy rockburst
12	Zhou et al. (2018b)	$\sigma_{\theta, max} / \sigma_c$ σ_T / σ_c $(\sigma_\theta + \sigma_T) / \sigma_c$	$\sigma_{\theta, max} / \sigma_c < 0.26$ None rockburst $0.26 \leq \sigma_{\theta, max} / \sigma_c < 0.33$ Light rockburst $0.33 \leq \sigma_{\theta, max} / \sigma_c < 0.47$ Medium rockburst $\sigma_{\theta, max} / \sigma_c \geq 0.47$ Heavy rockburst < 0.27 None rockburst $0.27 \leq * < 0.35$ Light rockburst $0.35 \leq * < 0.46$ Medium rockburst ≥ 0.46 Heavy rockburst < 0.30 None rockburst $0.30 \leq * < 0.44$ Light rockburst $0.44 \leq * < 0.58$ Medium rockburst ≥ 0.58 Heavy rockburst

Table 1 (continued)

Serial number	References	Index and/or equations	Intensity grading
13	He et al. (2020)	$\beta = \sigma_c \cdot (\sigma_{pmax} - \sigma^0) / (R_0 \cdot \sigma_{pmax})$ (pre-conditions: $\frac{\sigma_{max}}{\sigma_c} > 0.4$)	$\beta < 3.7$ Light rockburst $3.7 \leq \beta < 7.2$ Medium rockburst $7.2 \leq \beta < 8.7$ Heavy rockburst $\beta \geq 8.7$ Serious rockburst
14	Liu et al. (2021a)	$B_r = (\sigma_p - \sigma_r) / [\sigma_p (\epsilon_r - \epsilon_p)]$	-
15	Dat et al. (2022)	$Ker = P_m / P_{mcr}^*$	0 < SDR < 0.25 None rockburst 0.25 ≤ SDR < 0.50 Light rockburst 0.50 ≤ SDR < 0.75 Medium rockburst SDR ≥ 0.75 Heavy rockburst

criterion, etc. However, the application of rockburst discrimination criteria based on a certain index was found to be unsatisfactory, and it resulted in large prediction deviations, despite the advancement of engineering technology. For instance, Zhou et al. (2018b) tried to adopt these guidelines to discriminate the rockburst class of the Gaoligongshan tunnel. It was found that the various guidelines were independent of each other and applied to different engineering conditions. To establish the connectivity between indices σ_1/σ_c , $\sigma_{\theta,max}/\sigma_c$ and $(\sigma_{\theta} + \sigma_L)/\sigma_c$, Zhou et al. proposed a rockburst discrimination criterion based on these three indices, as shown in Table 1. However, there is still a lack of research on combining multiple discriminant indices for rockburst intensity classification.

By analyzing Table 1, it was found that the evaluation indexes established based on the maximum tangential stress of surrounding rock σ_{θ} , uniaxial compressive strength σ_c , uniaxial tensile strength σ_t and Stress coefficient σ_{θ}/σ_c are the majority. It indicates that the mechanical properties of the rock have a great influence on the occurrence of rockbursts. However, it should be noted that the stress method established based on strength theory ignores the dynamic characteristics of rockburst. It is easy to confuse general brittle damage with rockburst (He et al. 2023).

The occurrence of rockbursts is related to the mechanical properties of the surrounding rock and the stress transfer path (Liu et al. 2021c). Therefore, the empirical method that only considers the mechanical properties is not comprehensive. Some scientists consider the role of the stress gradient in the surrounding rock based on the stress–strength ratios criterion. They are establishing a new criterion based on stress–strength ratios and surrounding rock stress gradient, namely the SR-SG criterion (Liu et al. 2023c). The advantage of the SR-SG criterion is to improve the accuracy of prediction while overcoming the problem of inhomogeneity in the grading interval of traditional criterion indicators. Table 2 gives the application of the SR-SG criterion in rockburst intensity grading.

3.1.2 Energy methods

The rock mass generates strain energy in a plateau state of locational stress or a low-stress state of external disturbance. Accumulation of strain energy is generally recognized as the main energy source of rockburst, and the strain energy stored in the rock largely determines the intensity level of the rockburst (Li et al. 2007; He et al. 2023).

Figure 4 shows the general process of energy evolution inside the rock mass under external perturbation. Various external perturbation loads act on the rock body, resulting in

Table 2 Rockburst grading criteria based on the SR-SG criterion (Liu et al. 2023c)

TSGC/MPa m ⁻¹	Rockburst intensity			
	None	Light	Medium	Heavy
0–7.5	R < 0.20	R ≥ 0.20	–	–
7.5–12.5	R < 0.22	0.22 ≤ R < 0.44	R ≥ 0.44	–
12.5–20	R < 0.28	0.28 ≤ R < 0.60	0.60 ≤ R < 0.97	R ≥ 0.97
20–40	R < 0.33	0.28 ≤ R < 0.74	0.74 ≤ R < 1.50	R ≥ 1.50
> 40	R < 0.40	0.40 ≤ R < 2.00	R ≥ 2.00	–

TSGC: the tangential stress gradient coefficient of the surrounding rock, $TSGC = \sigma_1(7 - 5\lambda)/a$; λ : the lateral pressure coefficient, $\lambda = \sigma_3/\sigma_1$; a : the diameter of tunnel radius; R: the stress–strength ratios of the surrounding rock, $R = \sigma_{\theta,max}/\sigma_{ci}$

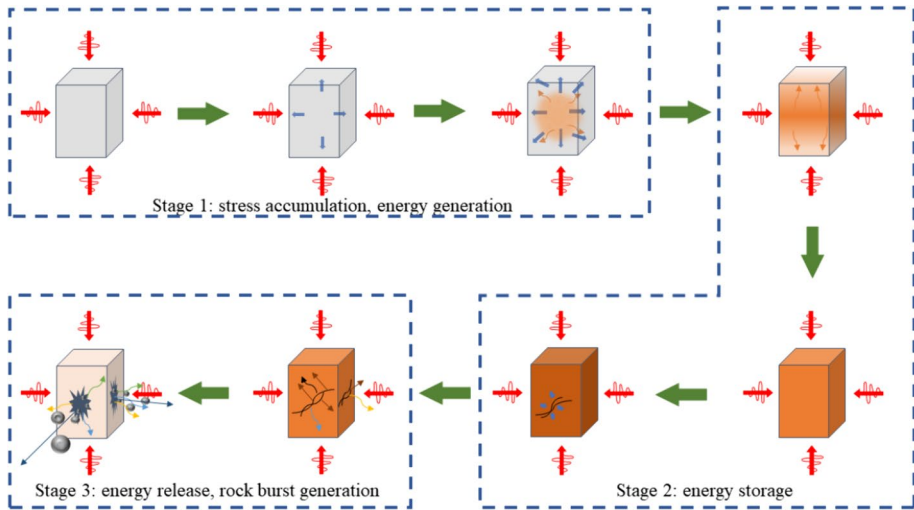


Fig. 4 General process of typical energy evolution

the generation of corresponding stresses inside the rock body to resist the external action. According to the law of conservation of energy, mechanical energy is input into the rock body’s interior and stored. When the energy stored inside the rock reaches the threshold of rockburst, the energy is actively released to the outside world. Once the crack is created afterward, some of the energy is converted into kinetic energy of the fragments, causing the rocks around the crack to be violently ejected and the rockburst occurs (Liu et al. 2013; Li et al. 2023b). Scholars have established a large number of rockburst evaluation indexes based on the energy evolution process. One of the most widely used indexes is the Wet index, which evaluates rock hardness, brittleness, and susceptibility to bursting.

Table 3 presents the empirical methods based on energy theory that have emerged in recent years, along with their associated discriminant and rockburst classifications. The rockburst phenomenon occurs when the external force acting on the rock reaches the limit of what the rock body can withstand. This phenomenon is observed both in the engineering field and in indoor tests. Therefore, studying the proportionality between the elastic strain energy density and the dissipated strain energy density at the peak intensity of a rock specimen may facilitate the assessment of rockbursts. Gong et al. (2019) proposed the W_{ET}^P index for rockburst intensity classification in this context, as shown in Table 3. The advantage of using the W_{ET}^P index is that it no longer calculates the strain energy density at the point of 80–90% of the peak intensity, making the index more suitable for actual use. Additionally, several scholars have proposed or improved the theoretical discriminant for the W_{et} index (Zhang et al. 2011; Wang et al. 2021d). Further in-depth research is needed to improve the accuracy of the rock burst criterion based on the energy theory.

The establishment of different energy methods is mainly based on the energy density and energy release rate at different stages of the rock fracture process. On the one hand, it confirms that energy evolution is an important factor in determining the magnitude of the rockburst intensity. On the other hand, it reflects that the energy methods consider the dynamic behavior of the energy evolution, such as the local energy release rate, while considering the static quantitative indicators. Gong et al. (2020) further verified that the energy methods have better predictive performance by comparing 20 tendency evaluation indices

Table 3 Summary of rock burst criteria based on energy theory and assessment of qualitative indicators for rockburst grading

Serial number	References	Index and/or equations	Intensity grading
1	Zhang et al. (2011)	$W_{ET} = U_{ET}^e / U_{ET}^d$	$W_{ET} < 2.0$ None rockburst $2.0 \leq W_{ET} < 3.5$ Light rockburst $3.5 \leq W_{ET} < 5.0$ Medium rockburst $W_{ET} \geq 5.0$ Heavy rockburst
2	Jin and Zhou (2012)	$E = W_E = 2 \times \omega_e \times V$	$E < 15.7$ None rockburst $15.7 \leq E < 39.25$ Medium rockburst $39.25 \leq E \leq 78.5$ Heavy rockburst $E > 78.5$ Serious rockburst
3	Deng et al. (2012)	$B_q = U_q^e / (U_q^e + U^a)$	$0 \leq B_q < 0.20$ None rockburst $0.20 \leq B_q < 0.50$ Light rockburst $0.50 \leq B_q < 0.80$ Medium rockburst $0.80 \leq B_q < 1.00$ Heavy rockburst
4	Qiu et al. (2014)	$\left[\frac{(U_{imax} - U_{imin})}{U_{imax}} \right] / [U_{max}(p)]$ $RERI = / [(U_{max}(p) - U_{res}(p))]]$	-
5	Keneti and Sainsbury (2018)	$BIM = U^0 / U_{BIM}^0$	$BIM > 1.50$ Light rockburst $1.50 \geq BIM > 1.20$ Medium rockburst $1.20 \geq BIM > 1.00$ Heavy rockburst
6	Gong et al. (2018b)	$A'_{CF} = U^e / U^a$ $A_{EF} = U^e - U^a$	- $A_{EF} < 50$ None rockburst $50 \leq A_{EF} < 150$ Light rockburst $150 \leq A_{EF} \leq 200$ Medium rockburst $A_{EF} > 200$ Heavy rockburst
7	Jiang et al. (2019)	$LERR = U_{imax} - U_{imin}$	-
8	Gong et al. (2019)	$W_{ET}^P = U_e / U_d$	$W_{ET}^P < 2$ None rockburst $2 \leq W_{ET}^P \leq 5$ Light rockburst $W_{ET}^P > 5$ Heavy rockburst
9	Zhang and Jiang (2020)	$U \geq U_h + U_d$ $\sigma_x \geq R_x \epsilon [s, l - s]$	-
10	Gao et al. (2020)	$W_p = K_{ED}^f / K_{ED}^p$	-
11	Wang et al. (2021d)	$W_{et} = \varphi_{sp} / \varphi_{st}$	$W_{et} < 2.0$ None rockburst $2.0 \leq W_{et} < 5.0$ Light rockburst $W_{et} \geq 5.0$ Heavy rockburst
12	Luo et al. (2023)	$LERE_i = (E_{imax} - E_{imin}) \times LERS_i^2$	-

such as the strain energy storage index, the energy impact index, the potential energy of elastic strain, the rockburst energy index, the deformation brittleness index, the brittleness index of rockburst proneness, the deformation modulus and the lag time ratio index, etc. However, the difficulty in determining and measuring the stress and strain fields has led to limitations in the use of energy methods in practice.

3.2 Empirical methods with multi-index indicators

Figure 5 summarises some of the factors that influence the occurrence of rockbursts. Some scholars have discussed the influence of size effect, rock material (rock type, rock properties, and structural planes), mechanical conditions (stress state, loading/unloading rate, and dynamic perturbations), and environmental conditions (moisture content and temperature) on rockburst by considering some of the influencing factors. It is shown that rockbursts are the result of a combination of factors (He et al. 2023). Therefore, the single indicator evaluation method developed by considering only factors such as rock mechanical properties or rock energy evolution has limitations. It is easy to apply different evaluation indicators to the same rock samples when the results of the dispersion of the situation.

The advantage of the comprehensive evaluation index is that multiple factors affecting rockburst are used as control factors for rockburst prediction. Breakthrough the single indicator evaluation method only considers the limitations of a single factor. Thus, the prediction accuracy and reliability of the empirical index method have been further improved.

Some scholars have carried out research by combining the mechanical properties of rocks and the evolution process of strain energy. The elastic modulus damage index (EMDI) based on peak stress dissipation energy U_d , peak stress total strain energy U , elastic modulus E , and peak strength σ_p is established by considering both strength theory and energy theory (Khan et al. 2022). EMDI is defined as in Eq. (1). When the EMDI value is less than 0.91 for no rockburst, greater than 1.93 for strong rockburst, between the middle range for weak rockburst. From the properties of the indicator, this approach has the distinctive feature of energy-feeding stress. The rockburst prediction is improved by combining the advantages of the energy methods with the disadvantages of the stress methods.

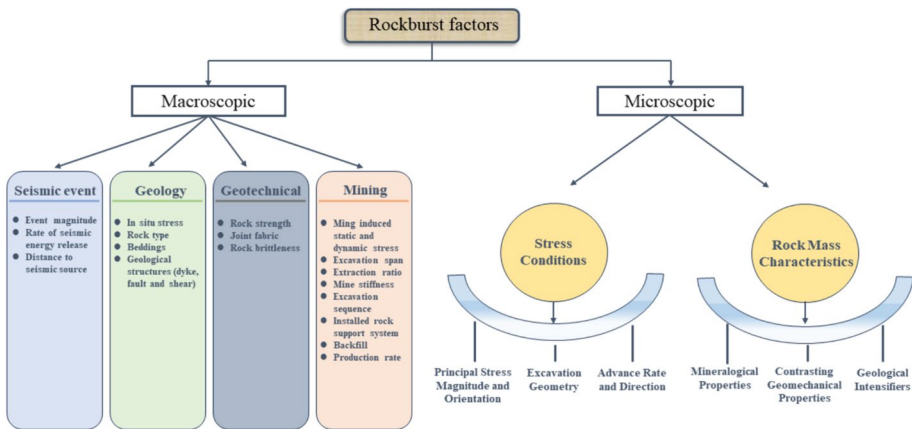


Fig. 5 Factors affecting rockburst (Modified according to Kaiser and Cai (2012) and Keneti and Sainsbury (2018))

$$\text{EMDI} = (\lambda/E) \cdot (U_d/U) \cdot (\sigma_r/\sigma_p) \quad (1)$$

At present, the methods that are used more in the comprehensive evaluation method for the assignment of each indicator include the fuzzy comprehensive evaluation method (FCE), principal component analysis (PCA), analytic hierarchy process (AHP), and quantitative evaluation method (QEM).etc. (Du et al. 2021). The advantage of these methods is that the weights of the indicators can be assigned scientifically. This makes the prediction results more accurate and reliable than single indicator evaluation methods. Zhang et al. (2020c) scientifically assigned weights to five indexes, namely uniaxial compressive strength σ_c , stress coefficient σ_θ/σ_c , brittleness coefficient of rock B_r , elasticity energy index W_{et} and rock mass integrity coefficient K_v , by adopting a comprehensive weight evaluation method combining AHP and variation coefficient methods, which comprehensively considered the factors of pathological stresses, lithological properties and energy conditions. A comprehensive index evaluation method based on the five indexes was established. Zhu et al. (2022) used a combination of AHP and FCE methods, considering the geodynamic environment, and geological and mining factors. A comprehensive evaluation index system was established based on 15 influencing factors, such as the dip angle of the tectonic depression, the ratio of the tectonic stress to the vertical stress, the vertical movement velocity of fault blocks, the influence zone of fault structure, the mining depth, the thickness variation coefficient of the coal seam, the uniaxial compressive strength and the collapse degree of overlying strata, and so on. The weights of the factors are scientifically determined, and the prediction results are more in line with the actual situation.

Once the tunnel is excavated, the rockburst evolution process manifests itself as a gradual release of radial stress and a gradual increase in tangential stress, forming a tangential stress concentration and inducing rock fragment ejection (Pan et al. 2020). On this basis, Hoek and Brown (1980) proposed a criterion for the stress-intensity ratio. However, a large number of evaluation indexes do not take into account the radial radius of the tunnel and the radius of the plastic zone. Later, a new comprehensive evaluation index ζ based on the stress-strength ratio criterion was proposed by Yang et al. (2022), which takes into account the radial stress σ_r^p , tangential stress σ_θ , tunnel radius r_0 , plastic zone radius r_p , and uniaxial compressive strength σ_c .

In recent years, some scholars have incorporated geological conditions and site construction status into the comprehensive evaluation system. A multi-indicator evaluation method based on in-situ stress, rock brittleness, elastic deformation energy, maximum storage elastic strain energy, rock integrity, groundwater condition, section design size, and site construction status was established by considering five aspects: rock mechanical properties, strain energy evolution, geological conditions, tunnel design parameters, and site construction conditions. Verified by engineering examples, the predicted results are in general agreement with the actual occurrence of rockburst (Qu et al. 2022).

With the continuous deepening of the theoretical study of rock burst prediction, from a single stress method or energy method to the comprehensive consideration of mechanical properties and strain energy evolution of the comprehensive method, and then to the establishment of the mechanical properties of the rock, the evolution of strain energy, geological conditions, tunnel design parameters and construction conditions of the site of the integrated evaluation system, the comprehensive indicators of the evaluation method has been gradually improved. Its prediction performance is gradually improved. It should be noted that although the weighting problem of each indicator is considered, the problem of nonlinear relationships between multiple indicators is not effectively solved. To a certain extent, this limits the predictive performance of the comprehensive indicator evaluation

method. In addition, the evaluation indicators should be selected according to specific problems and data characteristics, while weighing them against the requirements of practical applications.

4 Rockburst prediction methods based on dynamic indicators

In recent years, the focus of research has shifted from static indicators to dynamic indicators. The reason for this is that static indicators have to be obtained manually from indoor tests or field measurements. The process is relatively complicated and lacks continuity and timeliness. Dynamic indicators are obtained in real-time by the monitoring system and monitoring equipment, which has the advantages of data integrity, continuity, and timeliness (Du et al. 2021). microseismic monitoring (MS) and acoustic emission (AE) are the main in-situ monitoring methods for the common rockburst problems in tunneling (Mogani and Stacey 2019; Cheng et al. 2020).

4.1 Microseismic monitoring method

The MS monitoring technique has the advantages of low cost, wide monitoring range, high immunity to interference, no impact on on-site construction, and can relatively accurately determine the location and timing of rock microfracture events (Ma et al. 2016; Tian et al. 2022; Yang et al. 2023). Figure 6 shows a diagram of the microseismic monitoring system. The MS monitoring technology has gradually become one of the most effective tools in the field of rockburst monitoring since it was first introduced in China in 1959 for impact trend monitoring at the Mentougou coal mine (Li et al. 2007; Tang et al. 2015; Ma et al. 2016).

Tunneling causes disturbances in the surrounding rock mass (manifested as microseismic events, also known as rock fracture events). This causes a redistribution of stresses within the rock mass. The altered stress paths cause localized microcracking and damage to the rock close to the working face. This causes some of the internal energy to be released

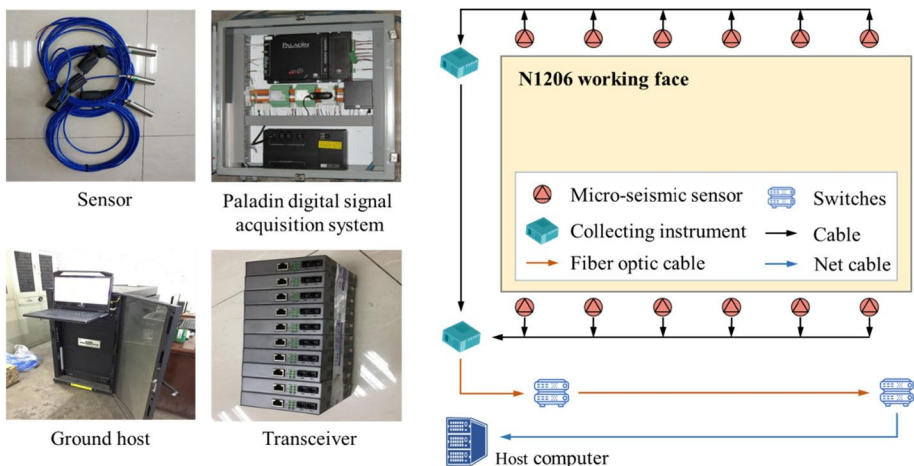


Fig. 6 Topology of the microseismic monitoring system. (Zhang et al. 2021)

outwards in the form of elastic waves (Zhang et al. 2018, 2020d). The frequency characteristics of various waves are shown in Fig. 7. MS system sensors receive a large number of signals simultaneously. These include MS signals (e.g., p-wave and s-wave) and noise signals such as electric current, knocking, rock drill, and locomotive whistle. Monitoring data is voluminous and complex, requiring effective processing and interpretation by professionals. The results are heavily influenced by environmental noise and interference. The MS signals are retained by the denoising process. Then, they are converted into electrical signals and uploaded to the analysis and warning center step by step. The analysis and warning center further analyze the source parameters and spatial distribution pattern of MS events to obtain rockburst precursor information. Finally, it is sent to the terminal to realize the effective prediction of rockburst (Mousavi and Langston 2016; Iqbal et al. 2018).

By analyzing the received elastic waves, a large number of microseismic source parameters (dynamic indicators) can be obtained, such as apparent stress (σ_A), apparent volume (V_A), p-wave arrival time, seismic energy density, microseismic event density, energy index (EI), 3S (stress accumulation, stress shadow and stress transfer) index, b value (b), and number of energetic tensile damage events (Cai et al. 2014; Dou et al. 2018; Ma et al. 2020; Yu et al. 2022). etc. Apparent stress, apparent volume, energy index, and microseismic energy (E) are commonly used dynamic warning indicators. Among them, the apparent volume reflects the size of cracks in the rock mass. The energy index reflects the pressure level of the rock mass. Microseismic energy reflects the intensity of microseismic events. The use of these indicators can effectively explain the state of cracks in the rock mass for real-time early warning of a rockburst. Xue et al. (2020a) proposed that $\lg N/b$ can be used as a new indicator for rockburst warning based on the number of microseismic events and b value. The larger the value of $\lg N/b$, the more serious the rockburst. Zhang et al. (2021) quantitatively analyzed the average release energy, apparent volume, b value, and s value to propose a new index the energy rockburst warning (ERW) index. Table 4 summarizes the early warning situation for selected indicators.

As mentioned above, each dynamic indicator has its theoretical formula. The differences between the indicators show that the development state of rock fracture can be interpreted from different aspects. Therefore, the comprehensive use of more source parameters to avoid the one-sidedness and limitation of a few indicators is an effective way to improve the accuracy of real-time warning (Feng et al. 2015; Wang et al. 2021e).

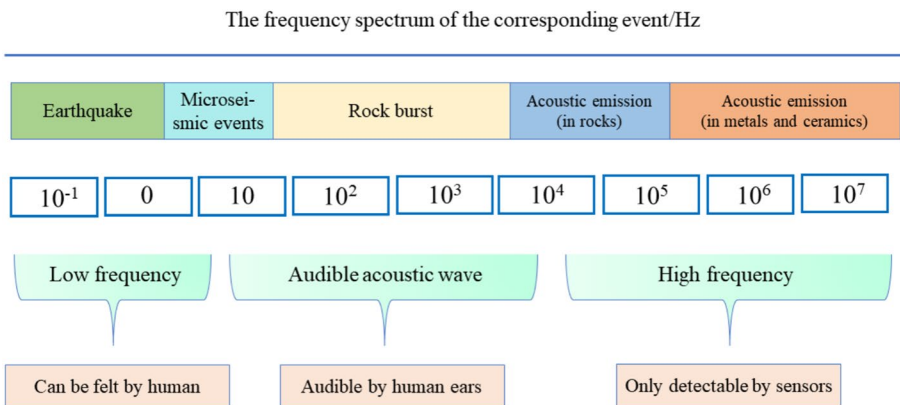


Fig. 7 Frequency characteristics of various waves (modified according to Su et al. 2017)

Table 4 Real-time dynamic early warning discriminations for selected microseismic indicators

Dynamic indicators	Theoretical formula	Real-time warning	Legend	References
E, σ_A, V_A, EI	$E = 4\pi\rho cR^2 \frac{J_c}{F_c}$ $\sigma_A = \frac{\mu E}{M_0}$	<p>Cumulative MS energy and cumulative apparent volume increase rapidly after the first rock burst. The energy index continues to rise. This indicates that a rockburst is about to occur. After the second rockburst, the cumulative MS energy and the cumulative apparent volume increase gradually. The energy index drops sharply. This indicates that a rockburst will not occur for some time</p>		Wang et al. (2021e)
EI, V_A, E	$V_A = \frac{M_0}{2\sigma_A}$	<p>On January 5, the energy index curve was more volatile. The increment of cumulative apparent volume is large. Reveals that a rockburst is imminent. on January 6, the increments of cumulative apparent volume and cumulative MS energy suddenly increased. A sudden decrease in energy index. Reveals that a rockburst is imminent</p>		Xue et al. (2020a)
V_A, EI, b	$EI = \frac{E}{E(M_0)}$ $\lg N = a - bM$	<p>Around December 15, 2019, the energy index and b value curves suddenly decreased. The cumulative apparent volume gradually increased. The rock mass enters the strain-softening phase and a large-scale microseismic event is about to occur. In early February 2020, the energy index decreased sharply again. B value decreases slowly. A large-scale rockburst did not occur</p> <p>On March 24 and 28, the energy index curve decreased sharply and the b-value curve decreased significantly. The cumulative apparent volume curve increased significantly. It indicates a sudden release of energy from the rock mass, revealing the occurrence of a rockburst</p>		Wang et al. (2023a)
				Du et al. (2022)

E is the energy released by microcracks; ρ is the rock density; c is the elastic wave velocity; R is the radius of the epicenter; J_c is the particle motion velocity integral; F_c is the empirical coefficient of seismic wave radiation type; M_0 is the seismic moment; μ is the rock shear modulus; $E(M_0)$ is the average seismic energy; N is the number of events with magnitude greater than M ; M is the magnitude; a and b are coefficients

Analyzing the cloud map of microseismic spatiotemporal distribution characteristics is another way to obtain information on rockburst precursors. Figure 8 shows the cloud map of spatio-temporal distribution characteristics of microseismic events in a section of the Qinling tunnel. From June 20 to 29, 2018, microseismic event density gradually increased. A red risk signal appeared on the 26th, with a high risk of rockburst. As of the 29th, the rockburst risk reached 90%, revealing that a rockburst is imminent (Ma et al. 2022b). Khan et al. (2023) proposed four microseismic precursor characterization indices, namely cumulative frequency, cumulative energy, energy deviation, and frequency deviation, from the time dimension. The spatial distribution of each microseismic precursor warning index is obtained from spatially distributed cloud density maps. A temporally and spatially integrated warning method is established based on the time and spatial dimensions to predict the probability of rockburst occurrence in a short period.

It should be noted that MS signals in field monitoring are mostly analyzed and processed based on individual subjective experience. To a certain extent, this can cause the deviation of rockburst precursor characteristics in time and space. Therefore, by further combining microseismic and artificial intelligence technologies to establish a more objective MS signal processing system, the predictive performance of rockburst precursor characteristics in time and space can be effectively improved.

4.2 Acoustic emission monitoring methods

AE is the phenomenon of transient elastic wave emission resulting from the rapid release of energy within a material. It allows monitoring of the surrounding rock before internal cracks propagate to the surface of the material (Zhang et al. 2015). Accurately localizing microcracks and stress changes within rock formations is crucial for assessing rock stability and fracture conditions. However, interpreting monitoring data requires experienced professionals and the accuracy and reliability of the results are affected by the operator's level of expertise. Figure 9 shows the topology of the AE system. According to the acoustic emission theory, the AE technique has a similar working principle to the MS technique. The difference is that the sensor receives acoustic signals rather than vibration signals generated by microcracks in the rock (Zhang et al. 2014). Since the AE technique was first applied to the study of rock damage in 1962 (Kiyoo 1962), the technique has achieved a large number of research results in fields such as coal mining and rock bursting. It has been widely used in geotechnical monitoring (Browning et al. 2017; Xiao et al. 2019; Tan et al. 2022).

In the paper on AE field monitoring methods, acoustic emission parameters, and waveform characterization are the main analysis methods. All AE signals can be covered by these two analysis methods, and AE dynamic indicators can be obtained (Li et al. 2017a). The AE parameter metrics include AE hit count, AE energy, ringer count, energy count, decay count, rise time, peak amplitude, b value, and number of acoustic emission rings (Ban et al. 2020; Ding et al. 2022; Dong et al. 2022). Among them, the AE hit count reflects the density and intensity of AE activities inside the rock mass, and the AE energy can accurately capture the fine fracture behavior inside the rock mass. The ring count reflects the crack width. b value changes reflect the trend of cracks inside the rock mass. The AE ring count can reflect the damage to the rock mass to a certain extent. Based on the above parameters, the stability of the rock during loading can be further investigated to analyze the precursor characteristics of rock explosion.

Hu et al. (2018) explored the rockburst process in the borehole by analyzing the AE hit count and AE energy. As shown in Fig. 10. Before the rockburst occurs, there is a quiet period in the AE hit count curve. This period has the remarkable characteristics of a sharp decrease in the AE hit count and a sharp increase in the AE energy. Therefore, the quiet period can be used as a precursor signal for the occurrence of a rockburst. Zhai et al. (2020) performed true triaxial compression experiments on granitic syenite to further validate the reasonableness of the quiet period as a warning signal for rockburst.

Wang et al. (2022) performed true triaxial compression tests on granite. Comparative analysis of AE impact counts, ringing counts, and AE energies revealed that the accelerated release characteristics of AE energies better reflect the precursor information of rockburst.

Ren et al. (2023) used marble rock samples to simulate static-driven rockburst, pulse-disturbance rockburst, and period-disturbance rockburst. On the one hand, it is proposed that the trend of multiple fractal parameter curves increasing and then decreasing near the peak intensity can be used for rockburst warning for long-term monitoring. The inflection point is used to calculate the warning time, and the higher the rockburst intensity, the

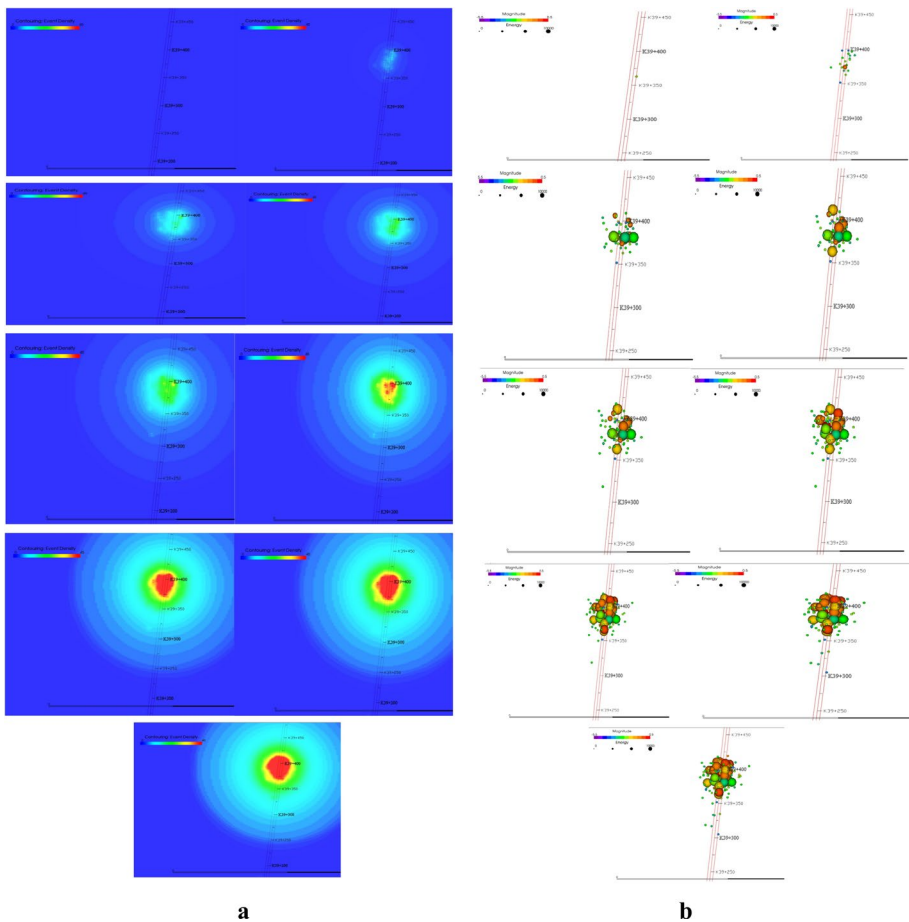


Fig. 8 Spatial and temporal distribution of microseismic events. **a** Density cloud map of microseismic events. **b** Map of microseismic events (Ma et al. 2022b)

shorter the warning time. On the other hand, it is verified that the stress drop can be used for short-term monitoring of rockburst warning.

The significant decrease in b value can be used as a precursor feature of rockburst, and the softening effect of water can significantly reduce the incidence of rockburst (Zhang et al. 2020e; Dong et al. 2022).

The above analysis of rockburst precursor characteristics from the perspective of AE parameters belongs to the time domain parameter analysis. Differently, the frequency domain waveform analysis explains the dynamic damage characteristics of microcracks inside the rock mass by mapping the AE waveform signal from the time domain to the frequency domain.

Mei et al. (2019) conducted uniaxial compression experiments on marble rock samples. The AE dominant frequency characteristics were analyzed for the entire rockburst process (dominant frequency is the frequency of the maximum amplitude in the two-dimensional spectrum, which is usually obtained by the fast Fourier transform (FFT)). As shown in Fig. 11, the two red dashed lines indicate the beginning and the end of the rockburst. The results show that the migration of the dominant frequency density region from the low-frequency domain to the relatively high-frequency domain, as well as the density of the dominant frequency distribution in the high-frequency domain before and after the rockburst can be used as a rockburst precursor characteristic signal.

Information entropy can effectively characterize information about the source of rupture within a rock mass. It is useful for research on rockburst prediction (Zhou and Li 2012). Figure 12 shows the main frequency entropy distribution of granite rock samples. The results show that the peak point A point before the sharp decrease of entropy can be used as a characteristic point for rockburst prediction.

As mentioned above, AE hit counts, AE energy, AE ringing counts, and primary frequency are the main dynamic indicators for conducting rockburst early warning. It should be noted that the differences in the degree of internal fracture of the rock are reflected by different indicators, resulting in inconsistency in the information proposed based on different indicators of rockburst precursors. It is prone to prediction misjudgment and prediction delay phenomenon. Therefore, the further establishment of a multi-indicator synergistic prediction method can significantly improve the accuracy of rockburst prediction. In addition, due to the limitations of AE sensors and the influence of the test environment at the current stage, the AE dynamic parameters cannot reflect the essential characteristics of rock damage (Chai et al. 2018). The waveform signal contains all the information on

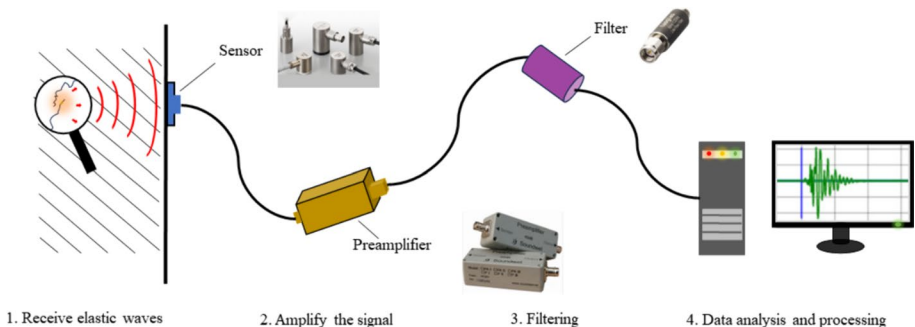


Fig. 9 AE monitoring system topology

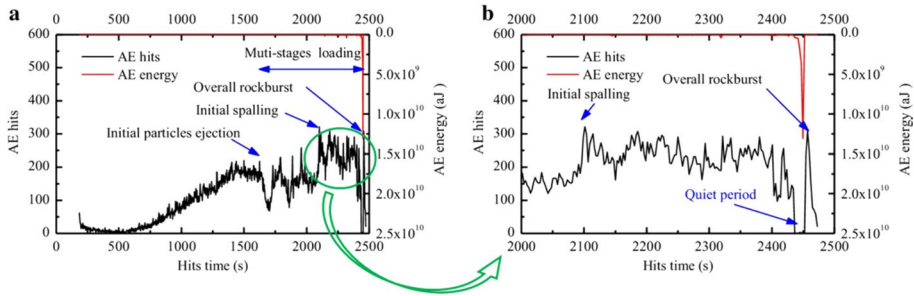


Fig. 10 Time series characterization of AE hit counts and AE energy. **a** Complete process. **b** The process of debris spalling to the occurrence of rockburst (Modified according to Hu et al. 2018)

mechanical properties and structural state inside the rock mass, which can better reflect the evolution of microcracks. Therefore, the rockburst precursor signal based on frequency domain waveform analysis is more reliable (Zhou et al. 2019; Zhu and Deng 2023).

Combined consideration of time domain parameters and waveform characteristics. To a certain extent, the combination of AE parameter signals and AE waveform signals to jointly implement rockburst precursor warning can avoid the errors caused by using one type of signal alone. Gao et al. (2023) verified that AE energy, AE ringing counts, and AE main frequency can be used as rockburst precursor signals. At the same time, they were defined as the key disaster-causing factors of rockbursts, to establish a comprehensive early warning method for brittle rockbursts. The initial warning point and key warning point of rock explosion were further obtained. As shown in Fig. 13.

5 Machine learning methods

Machine learning methods have the characteristic of discovering the change rule from a large amount of data and extracting the corresponding features (Marsland 2015). It can effectively extract the features related to the occurrence of rockburst from static and dynamic index data. For example, geological structure, stratum lithology, stress state, seismic activity, surface deformation, and so on. In addition, machine learning methods can make predictions based on real-time monitoring data. It can respond to rock changes and stress accumulation on time. It has a wide application potential in real-time rockburst prediction and monitoring systems. With the rapid development of big data science, the use of machine learning methods for rockburst prediction is gradually becoming a popular way (Pu et al. 2019b).

In recent years, numerous machine learning methods have been developed that use static and dynamic indicators as data inputs. Table 5 summarizes the use of static indicators as input data for machine learning methods in rockburst intensity classification in recent years. The table shows that σ_θ , σ_c , σ_t , and W_{et} are the earliest major static indicators used for machine learning in rockburst prediction, with prediction accuracies above 90%. The text suggests that the tangential stress, uniaxial compressive strength of rock, tensile strength of rock mass, and strain elasticity energy index W_{et} are advantageous in predicting rockburst and are highly applicable to certain algorithms. The field of rockburst prediction has seen the introduction of various new algorithmic models with the development

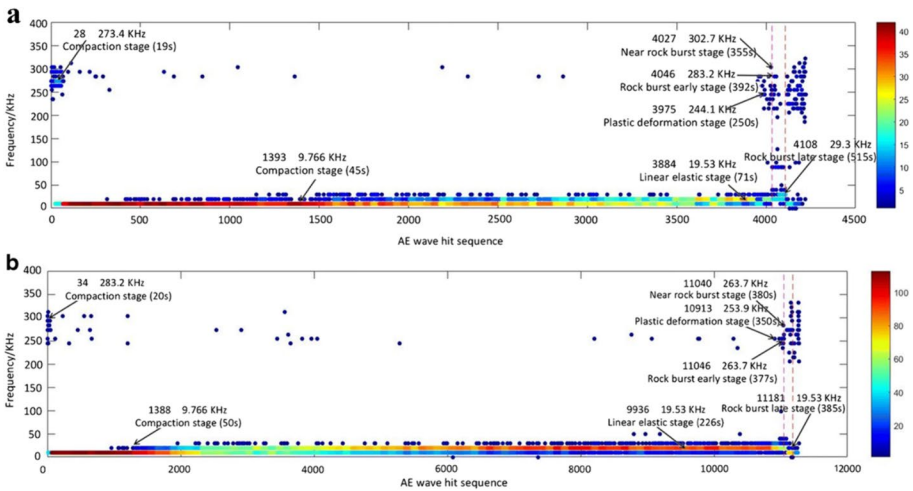


Fig. 11 Scattering density plot of AE full-time domain main frequency characteristics. **a** N5 sample. **b** N7 sample. (Modified according to Mei et al. 2019)

of computer engineering. It was determined that using only σ_θ , σ_c , σ_t , and W_{et} as input data did not yield satisfactory results for predicting rockburst. Therefore, scholars added the brittleness index σ_c/σ_t and stress concentration factor σ_θ/σ_c to the existing σ_θ , σ_c , σ_t , and W_{et} index to improve the prediction accuracy.

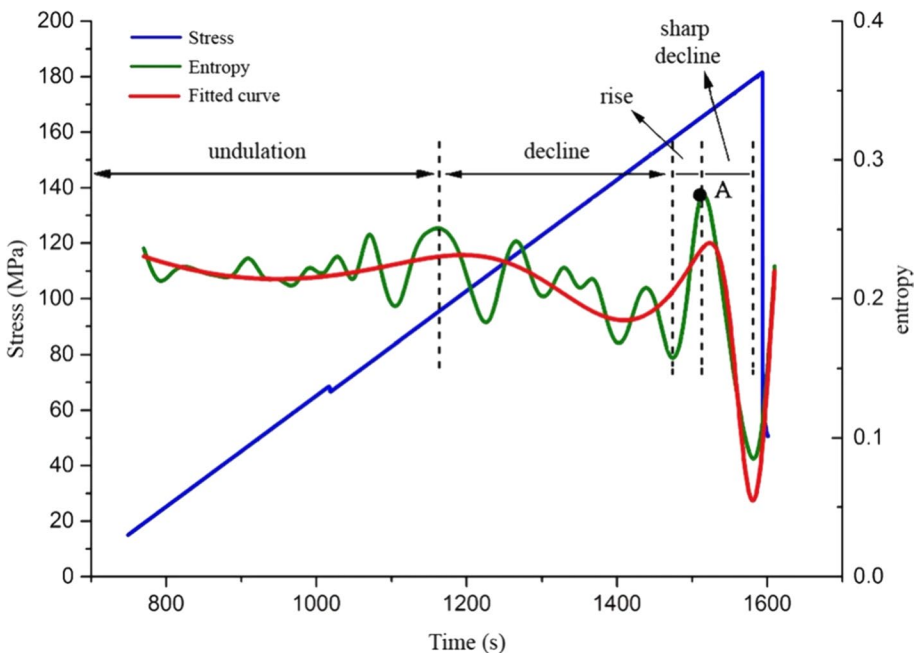


Fig. 12 Distribution of dominant frequency entropy of granite rock samples (Wang et al. 2021b)

The machine learning methods use maximum tangential stress σ_θ , compressive strength σ_c , tensile strength σ_t , brittleness index $\frac{\sigma_c}{\sigma_t}$, Stresscoefficient σ_θ/σ_c and elastic energy index W_{et} as common static inputs. σ_θ reflects the characteristics of the ground stress. Rocks are dense inhomogeneous bodies, and their lithological characteristics are reflected by σ_c and σ_t . Accumulation of strain energy is generally recognized as the main energy source of rockburst, W_{et} can reflect the ability of the rock to store strain energy. σ_c/σ_t and σ_θ/σ_c also have a close relationship with the intensity level of rockburst (Li et al. 2023a). Therefore, these indicators are more representative in explaining rockburst than other static indicators such as tunnel burial depth H and stress concentration factor SCF. Li and Jimenez (2017) and Li et al. (2022b) analyzed and found that W_{et} is always the most important indicator for rockburst prediction. As shown in Fig. 14.

Table 6 summarizes the use of dynamic metrics as input data for machine learning methods for rockburst intensity classification in recent years. The table shows that the machine learning method based on dynamic parameters can carry out rockburst warning, signal identification, crack identification, microseismic source localization, and p-wave first arrival time pickup. The dynamic parameter-based machine learning method offers greater degrees of freedom, as reflected to a certain extent. Currently, machine learning methods primarily utilize microseismic energy, seismic moment, cumulative number of events, cumulative apparent volume, and apparent stress as the main dynamic input indicators. Microseismic energy reflects the intensity of microseismic events to some extent. Seismic moment reflects the magnitude of the earthquake. Cumulative event count indicates the number and density of microfractures occurring within the rock mass. Cumulative apparent volume reflects the size of the cracks in the rock mass. Apparent stress indicates the degree of stress release (Liu et al. 2021b; Yin et al. 2021b).

The establishment of the indicator database is mainly based on the static and dynamic indicators obtained from global rockburst cases, rock indoor tests, numerical simulations, or field monitoring. At present, scholars have carried out the following studies to address the problems of the original database (Zhang et al. 2020b; Yin et al. 2021c; Zhou et al. 2021):

- (1) The number of rockburst cases in each class is disproportionate, causing the model to focus too much on the larger number of classes.

There are two main approaches to solving such problems. One is to oversampling, undersampling, or mixedsampling the data. The other is to replace algorithmic models that are insensitive to unbalanced data sets (Gnip et al. 2021). Xue et al. (2022) The

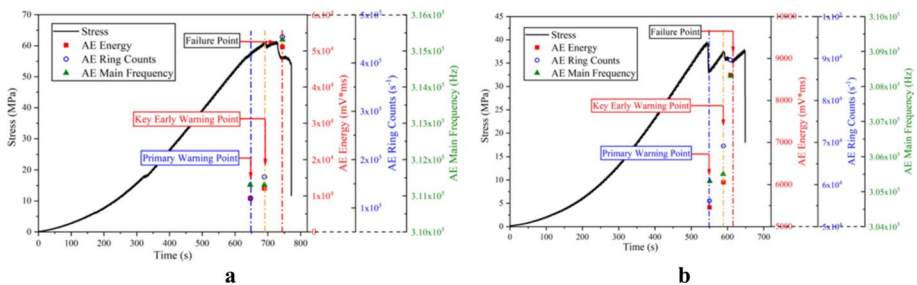


Fig. 13 Integrated rock burst warning method based on key causative factors of acoustic emission signals. **a** rock sample 1. **b** rock sample 2 (Gao et al. 2023)

Copula-MC oversampling algorithm is proposed based on Copula theory and Monte Carlo simulation. Through the validation of six machine learning models, the Copula-MC oversampling algorithm performs better than the synthetic minority oversampling algorithm (SMOTE) in dealing with unbalanced datasets, and the accuracies of each model are shown in Fig. 15. The Copula-MC oversampling algorithm significantly reduces the impact of unbalanced datasets on machine learning.

Li et al. (2022b) used the SMOTETomek algorithm to process the unbalanced dataset. Meanwhile, the BO-SMOTETomet-FNN model was established by combining bayes optimization (BO) and feedforward neural network (FNN). After engineering validation, the rockburst prediction accuracy reached 90.4%.

- (2) The model ignores other valuable information in the prediction process and overly relies on certain metrics. This leads to a decrease in the model's ability to predict new data.

The t-distributed Stochastic Neighborhood Embedding (t-SNE) (Van der Maaten and Hinton 2008) is a dimensionality reduction technique that effectively reduces the dependency between the parameters of each indicator. Pu et al. (2019b) combined the t-SNE technique and k-mean clustering with a support vector classifier (SVC). An SVC model based on the t-SNE technique and k-mean clustering was developed. And tenfold cross-validation was used to optimize the accuracy of this model to avoid overfitting. The results show that the model predicts well while reducing the indicator dependency. Feng et al. (2019) used a mean influence value algorithm (MIVA) to reduce indicator dependence and established a probabilistic neural network model for rockburst early warning.

- (3) Data Outliers. Data outliers are currently handled in three ways, namely removal, replacement, and transformation.

The Yeo-Johnson transform (He and Zheng 2018) preserves anomalous data. Reduces the impact of anomalous data on the overall prediction results and avoids the destruction of the original characteristics of the data when removing and replacing outliers. Sun et al. (2022) first used Yeo-Johnson transform to solve the outlier problem. Then k-mean SMOTE algorithm is used for oversampling to solve the unbalanced dataset problem, and PCA dimensionality reduction is used to reduce the indicator dependency problem.

- (4) Incomplete dataset due to missing data.

Liu et al. (2023a) proposed a histogram gradient boosting tree (HGBT) model for incomplete datasets. The model separates the samples from the missing values based on the potential gain at the point after finding the segmentation point, thus processing the missing values. By comparing seven models such as random forest (RF), K-nearest neighbors (KNN), extreme gradient boosting (XGBoost), support vector machines (SVM), and artificial neural network (ANN), the results show that the HGBT model has 77.78% prediction accuracy. The prediction performance is better compared to other models as shown in Fig. 16.

- (5) The issue of weighting of indicators.

Li et al. (2023c) used Tent chaotic mapping and the crossover and mutation operators in the genetic algorithm (GA) to improve the Harris Hawk (HHO) algorithm to obtain the IHHO algorithm, which is capable of assigning weights to indicators more objectively. By comparing with optimization algorithms such as GA and HHO, the IHHO algorithm has higher search efficiency and faster convergence accuracy. The

Table 5 Machine learning methods using static indicators as input data

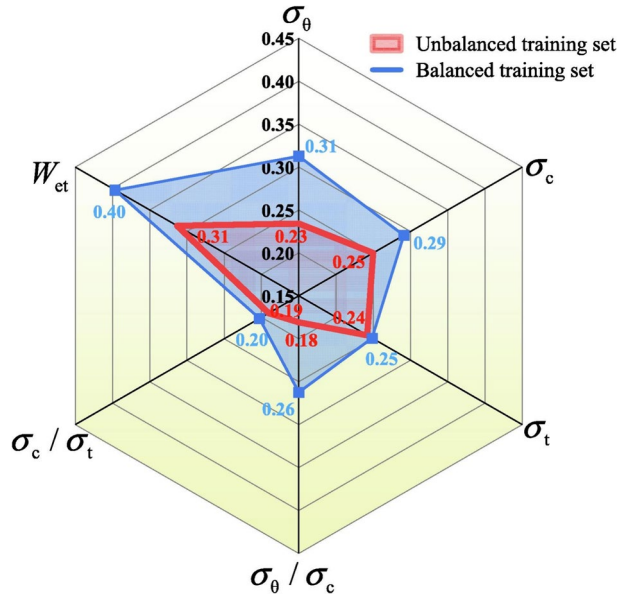
Machine learning methods	Static indicators	Data volume	Accuracy %	References
Random forest	$\sigma_\theta, \sigma_\theta, \sigma_c, \sigma_r, W_{et}$	46	100	Dong et al. (2013)
Random forest	$D, \sigma_\theta, \sigma_c, \sigma_r, \sigma_\theta / \sigma_c, \sigma_c / \sigma_r, (\sigma_c - \sigma_r) / (\sigma_c + \sigma_r), W_{et}$	246	71.18 48.86	Zhou et al. (2016)
Partial least-squares discriminant analysis			64.62	
Support vector machine	$\sigma_\theta, \sigma_c, \sigma_r, W_{et}$	30	69.33	Li et al. (2017c)
Gradient boosting machines	$H, \sigma_\theta, \sigma_c, \sigma_r, W_{et}$	135	95.0	Li et al. (2017b)
Extreme learning machine	$\sigma_\theta, \sigma_c, \sigma_r, W_{et}$	108	-1.85	Pu et al. (2018)
Naïve bayes	$\sigma_\theta, \sigma_c, \sigma_r, SCF, B_1, B_2, W_{et}$	246	95.0	Pu et al. (2019b)
Support vector machine	$\sigma_\theta / \sigma_c, \sigma_c / \sigma_r, W_{et}$	174	-	Ghasemi et al. (2019)
Support vector machine	$\sigma_\theta / \sigma_c, \sigma_c / \sigma_r, W_{et}$	58	90.23	Faradonbeh et al. (2020)
Decision tree-based C5.0 algorithm	$\sigma_\theta, \sigma_c, \sigma_r, W_{et}$		100	
Self-organizing map			75.86	
Fuzzy c-mean algorithms	$H, \sigma_\theta, \sigma_c, \sigma_r, W_{et}$	188	70.0	Zhang et al. (2020b)
Back propagation neural network			66.0	
Support vector machine			59.0	
Decision tree			63.0	
K-nearest neighbor			41.0	
Logistic regression			38.0	
Multiple linear regression			48.0	
Naïve bayes			80.0	
Integrated model based on 7 classifiers			-	
Extreme learning machine	$\sigma_\theta, \sigma_c, \sigma_r, \sigma_\theta / \sigma_c, \sigma_c / \sigma_r, W_{et}$	344		Xue et al. (2020b)
Artificial neural networks	$\sigma_\theta, \sigma_c, \sigma_r, \sigma_\theta / \sigma_c, \sigma_c / \sigma_r, W_{et}$	246	83.34	Zhou et al. (2020)
Extreme gradient boosting	$\sigma_\theta, \sigma_\theta / \sigma_c, \sigma_c / \sigma_r, W_{et}$	50	93.3	Xie et al. (2020)
Random forest	$H, \sigma_\theta, \sigma_c, \sigma_r, W_{et}$	279	92.0	Sun et al. (2021a)
Naïve bayes	$\sigma_\theta, \sigma_r, W_{et}$	134	94.78	Ke et al. (2021)
Firefly algorithm and random forest	$H, \sigma_\theta, \sigma_c, \sigma_r, W_{et}$	279	91.0	Sun et al. (2021b)
Scorecard	$\sigma_\theta, \sigma_c, \sigma_r, \sigma_\theta / \sigma_c, \sigma_c / \sigma_r, W_{et}$	311	75.0	Wang et al. (2021c)

Table 5 (continued)

Machine learning methods	Static indicators	Data volume	Accuracy /%	References
Radial basis function neural network	$\sigma_\theta/\sigma_c, \sigma_r/\sigma_r, W_{et}$	80	96.25	Gao et al. (2021)
Extreme gradient boosting	$\sigma_\theta, \sigma_c, \sigma_r, W_{et}$	134	96.3	Shukla et al. (2021)
Decision tree			100	
Support vector machine			88.8	
Deep forest	$\sigma_\theta, \sigma_c, \sigma_r, \sigma_\theta/\sigma_c, \sigma_c/\sigma_r, W_{et}$	344	90.8	Guo et al. (2021b)
Back propagation neural network—Support vector machine	$\sigma_\theta, \sigma_c, \sigma_r, \sigma_\theta/\sigma_c, \sigma_c/\sigma_r, W_{et}$	420	97.5	Guo et al. (2022)
Analytic hierarchy methods—random forest	$\sigma_\theta/\sigma_c, \sigma_r/\sigma_r, W_{er}, E_S, K_r, W, D, S$	20	90.0	Qu et al. (2022)
Feedforward neural network	$\sigma_\theta, \sigma_c, \sigma_r, \sigma_\theta/\sigma_c, \sigma_c/\sigma_r, W_{et}$	314	90.4	Li et al. (2022b)
Decision tree	$\sigma_\theta, \sigma_c, \sigma_r, W_{et}$	243	82.0	Xue et al. (2022)
Discriminant analysis			80.9	
Naïve bayes			81.2	
Support vector machine			88.9	
K-nearest neighbors			87.1	
Deep forest	$\sigma_\theta, \sigma_c, \sigma_r, \sigma_\theta/\sigma_c, \sigma_c/\sigma_r, W_{er}, (\sigma_c - \sigma_r)/(\sigma_c + \sigma_r)$	329	92.4	Li et al. (2022a)
Support vector machine	σ_c, UTS, BI, E, v	40	87.5	Liu and Li (2023)
Extreme learning machine	$\sigma_\theta/\sigma_c, \sigma_r/\sigma_r, W_{et}$	136	94.12	Li et al. (2023c)
Histogram gradient boosting tree	$\sigma_\theta, \sigma_c, \sigma_r, \sigma_\theta/\sigma_c, \sigma_c/\sigma_r, W_{et}$	314	88.9	Li et al. (2023a)
Convolutional neural network	$\sigma_\theta, \sigma_c, \sigma_r, \sigma_\theta/\sigma_c, \sigma_c/\sigma_r, W_{et}$	114	91.0	Li et al. (2023d)
Incremental learning– Naïve bayes	$\sigma_\theta, \sigma_c, \sigma_r, \sigma_\theta/\sigma_c, \sigma_c/\sigma_r, W_{et}$	382	92.9	Zhang et al. (2024)

D is the section design size; SCF is the stress concentration factor; E_S is the maximum storage elastic strain energy, $E_S = \sigma_c^2/2E$; W is the groundwater condition; S is for site construction; UTS is the ultimate tensile strength

Fig. 14 Importance analysis of static indicators (Li et al. 2022b)



extreme learning machine (ELM) model built based on the IHHO algorithm has better prediction performance.

Machine learning methods require a large amount of data to participate in training and testing, but the data sets used in machine learning are generally small at present, which reduces the robustness of the algorithmic model to a certain extent. Decision tree (DT) and naïve bayes (NB) models have better applicability to small samples, but the generalization performance is poor and cannot fundamentally eliminate the limitations of small samples (Li et al. 2017b; Ghasemi et al. 2019). In the future, there is a need to build a larger number of databases with higher quality and from a wider range of sources.

Machine learning methods show significant advantages in integrating multiple metrics and data processing, but they are susceptible to model limitations. For example, SVM algorithms are sensitive to sample perturbations, and the presence of high variance and low bias makes the prediction results lack generalization and robustness. For small samples, logistic regression (LR) is more prone to transition fitting. Ensemble learning methods can significantly improve the accuracy, stability, and robustness of prediction by integrating multiple algorithmic models. To a certain extent, it can make up for the shortcomings of single machine learning methods (Sagi and Rokach 2018; Zhang et al. 2020a). For example, Zhang et al. (2020b) used static indicators as input data and combined seven classifiers such as back propagation neural network (BPNN), support vector machine, decision tree, k-nearest neighbors, logistic regression, multiple linear regression (MLR) and naïve bayes to build an integrated BPNN-SVM-DT-KNN-LR-MLR-NB model. Liang et al. (2021) developed an integrated LR-NB-GP-MLPNN-SVM-DT model that combines six basic classifiers, namely logistic regression, naïve bayes, Gaussian process (GP), multilayer perceptron neural network (MLPNN), support vector machine and decision tree, using dynamic indicators as input data. The results all show that the prediction performance of the integrated classifier is better than the six basic classifiers.

Table 6 Machine learning methods using dynamic indicators as input data

Machine learning methods	dynamic indicators	Data volume	Accuracy /%	Appliance	References
Optimized probabilistic neural network	(1) Cumulative number of events (2) Cumulative energy (3) Cumulative apparent volume (4) Event rate (5) Energy rate (6) Apparent volume rate	93	100	Early warning of rock-burst risk based on microseismic data	Feng et al. (2019)
Short-term average and long-term average ratio	Raw MS waveform signal data	Case 1: 1760 Case 2: 5403 Case 3: 2223	Microseismic event recognition (Case 1: 85.98, Case 2: 92.45, Case 3: 91.06) Noise filtering (Case 1: 72.06, Case 2: 83.11, Case 3: 49.87)	Rupture signal identification is based on a large number of waveform signals. Filtering of non-ruptured signals	Chen et al. (2019)
Support vector machine	(1) Seismic moment	100	91.95	Recognizing microseismic and blasting events	Pu et al. (2020)
Back propagation neural network	(2) Microseismic energy		96.49		
Gaussian process model	(3) Number of trigger sensors		89.00		
Decision tree	(4) First peak amplitude		92.46		
Naïve bayes	(5) Maximum peak arrival time		93.16		
K-nearest neighbors	(6) Dominant frequency		97.02		
Logistic regression			97.54		
Adaptive boosting			96.49		
Random forest			95.27		
Gradient boosting machines			96.15		

Table 6 (continued)

Machine learning methods	dynamic indicators	Data volume	Accuracy /%	Appliance	References
Random forest	(1) Cumulative number of events	93	80.00	Comparing the predictive performance of five machine learning methods for short-term rockburst prediction	Liang et al. (2020b)
Adaptive boosting	(2) Cumulative energy		66.67		
Gradient boosted decision tree	(3) Cumulative apparent volume		76.67		
Extreme gradient boosting	(4) Energy rate		73.33		
LightGBM	(5) Apparent volume rate		66.67		
Convolutional Neural Network	Original AE event	3227	78.028	Pick up the first arrival time of the p-wave based on the original waveform trace	Guo et al. (2021a)
Artificial neural networks	(1) Number of events (2) Microseismic energy (3) Apparent volume	74	93.33	Early warning of rockburst risk based on microseismic data	Liu et al. (2021b)
Pruning precursor tree	(1) Seismic moment (2) Microseismic energy (3) Apparent volume (4) Apparent stress (5) Stress drop	300	98.90	Early warning of rockburst risk based on microseismic data. It is also shown that pruning the precursor tree improves the identification of a few categories in unbalanced datasets	Yin et al. (2021b)

Table 6 (continued)

Machine learning methods	dynamic indicators	Data volume	Accuracy /%	Appliance	References
Tree augmented naïve bayes	(1) Seismic moment (2) Microseismic energy (3) Source radius (4) Apparent stress (5) Stress drop	114	85.71	Combined microseismic monitoring techniques and naïve bayes networks for dynamic monitoring	Li et al. (2021)
Recurrent neural networks	Crack-induced electro-magnetic radiation data series	15,647	/	Recognize rockburst precursor signals and realize rockburst intelligent warning	Di and Wang (2021)
Convolutional Neural Network	(1) Microseismic energy (2) Seismic moment (3) Apparent volume (4) Apparent stress (5) Stress drop	400	91.67	Early warning of rockburst risk based on microseismic data	Yin et al. (2021a)
Logistic regression	(1) Cumulative number of events	91	76.67	Comparison of basic and integrated learners based on microseismic data	Liang et al. (2021)
Naïve bayes	(2) Cumulative energy		73.33		
Gaussian process	(3) Cumulative apparent volume		70.00		
Multilayer perceptron neural network			66.67		
Support vector machine			40.00		
Decision tree			63.33		
Integrated learner based on 6 learners			83.33		

Table 6 (continued)

Machine learning methods	dynamic indicators	Data volume	Accuracy /%	Appliance	References
Gaussian process	(1) Peak amplitude (2) VMD-based SampEn	600	97.60	Identification of tensile and shear cracks based on acoustic emission data	Jiang et al. (2022)
K-nearest neighbors	(1) Cumulative number of events (2) Event rate (3) Cumulative energy (4) Total daily energy (5) Cumulative apparent volume (6) Apparent volume	93	96.00	Early warning of rock-burst risk based on microseismic data	Kamran et al. (2022)
Non-linear support vector machine	(1) Cumulative number of events (2) Cumulative seismic energy (3) Cumulative apparent volume (4) Event rate (5) Seismic energy rate (6) Apparent volume rate	107	86	Early warning of rock-burst risk based on microseismic data	Jin et al. (2022)
Fully convolutional neural network	Raw MS waveform data	736	Positioning error < 5m	Microseismic source localization based on microseismic data	Ma et al. (2022a)

Table 6 (continued)

Machine learning methods	dynamic indicators	Data volume	Accuracy /%	Appliance	References
Multilayer perceptron	(1) Cumulative number of events	289	87.50	Early warning of rockburst risk based on microseismic data while comparing the prediction performance of six machine learning methods	Ma et al. (2023)
Support vector machine	(2) Cumulative energy		89.00		
Random forest	(3) Cumulative apparent stress		90.60		
Adaptive boosting	(4) Cumulative apparent volume		91.10		
Gradient boosted decision tree	(5) b value		89.60		
Extreme gradient boosting	(6) Maximum moment magnitude		93.80		
	(7) Absolute value of maximum displacement				
Moth flame optimization—support vector machines	(1) Angular frequency ratio (2) Cumulative energy (3) Apparent stress (4) Source radius (5) Energy ratio (6) Seismic moment	343	95.59	Early warning of rockburst risk based on microseismic data	Zhou et al. (2023)

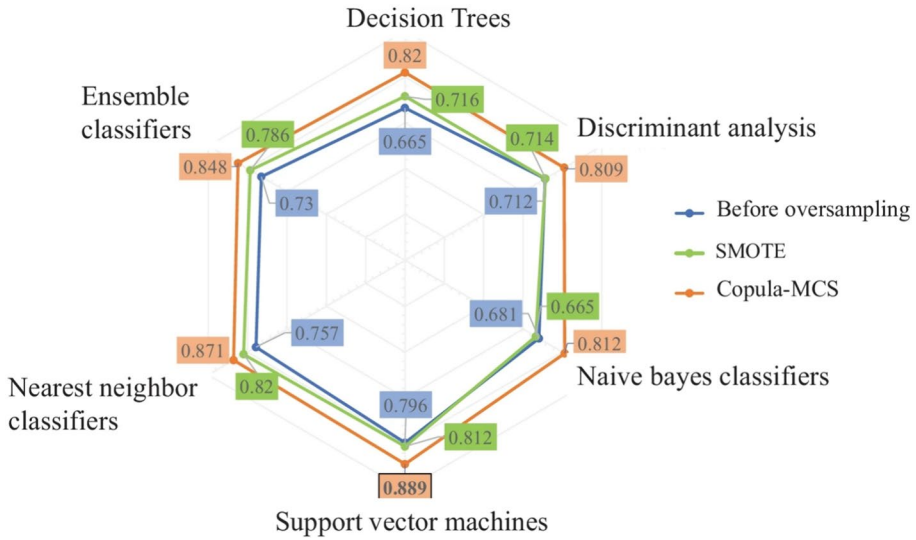


Fig. 15 Radar plot of different model predictions (Xue et al. 2022)

Deep learning methods are mainly based on the concept of artificial neural networks, which simulate the workings of the human brain through a multilevel network of neurons (Strawn 2022). Deep learning models can make full use of the information and patterns in the data by training and learning from large-scale data, thus improving the accuracy and generalization of predictions. Commonly used deep learning models include multi-layer perceptron (MLP), deep forests (DF), convolutional neural networks (CNN), temporal convolutional networks (TCN), recurrent neural networks (RNN), and long-short-term memory networks (LSTM). CNN can effectively deal with the temporal and spatial dependencies in the dataset. Therefore, it is widely used in microseismic monitoring. Yu et al. (2019) used microseismic raw waveform data as CNN input data to realize adaptive denoising. Song et al. (2020) used a CNN model to extract microseismic signals from blasting vibration signals to improve microseismic source localization accuracy. Peng et al. (2021) added Inception structures to the CNN model to form a deep CNN-Inception model for recognizing effective microseismic signals.

Attention is drawn to the fact that TCN models can handle the entire time series simultaneously, thus saving computational time. In addition, the TCN model can effectively deal

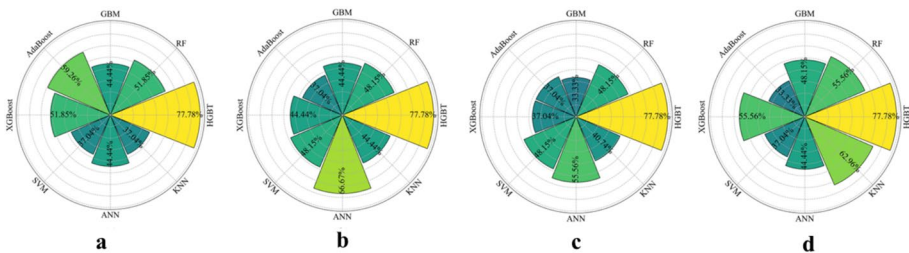


Fig. 16 Comparison of incomplete database models. Missing data is populated by the following values: a) 0; b) Average value; c) Median value; d) Common value (Liu et al. 2023a)

with the long-term dependence among indicators by capturing the time dependence of different ranges. Therefore, the application of TCN models in the field of rockburst prediction should be enhanced in the future.

6 Limitations and prospects

Empirical methods, microseismic monitoring, acoustic emission, and machine learning are four widely used methods for rockburst prediction. However, due to the complexity of the rockburst mechanism and the uncontrollability of the influencing factors, some aspects of them have some shortcomings and need to be improved in the future.

The empirical methods are a typical traditional rockburst prediction method. Its prediction process relies heavily on the criterion formula established by static indicators, which leads to at least two limitations of the empirical methods. For static parameters, a large number of single-indicator criteria consider only two or three factors, while the occurrence of rockburst is the result of a combination of factors, involving the mechanical properties of the rock mass, geological structure, digging methods, groundwater conditions, tunnel size and depth, etc. It is still unclear which factors are the most important. Thus the criterion formulae established by considering only a small number of factors have serious prediction errors. Even with the comprehensive indicator evaluation method considering multiple factors, the nonlinear relationship between the factors is difficult to determine. In the future, we should further study which factors play a dominant role in the process of rockburst occurrence, and at the same time consider more factors in the establishment of rockburst criterion. What is the relationship between rock tectonic properties, such as rock mineral composition, original pore state and texture orientation, and rockburst still needs to be further explored. In terms of criteria, each criterion formula has its rockburst grading standards. Therefore, the use of different criteria for the prediction of the same rockburst is prone to different rockburst grades, and a large number of criteria are uneven grading interval, resulting in rockburst intensity level imbalance. To a certain extent, this has increased the difficulty of accurate prediction of rockburst. In the future, the establishment of indicators should focus on how to build a uniform grading interval. The establishment of a unified and common rockburst criterion is still a long way to go.

Microseismic monitoring and acoustic emission are the two main field monitoring methods. A large number of waveform signals are often released before and after a rockburst. Whether the waveform signals received by the sensors are generated by the corresponding rupture event, or whether the sensors can segment the signals after receiving them overlapped together. Taking acoustic emission as an example, the overlapping of elastic wave signals leads to a decrease in the AE hit rate, but the cumulative AE counts and energy are increasing exponentially. This anomaly reduces the accuracy of AE monitoring to some extent. Therefore the problem of elastic wave signal overlap needs further study by scholars. A large number of dynamic indicators can be obtained by analyzing the elastic wave signals, such as p-wave arrival time, microseismic energy density, energy index, 3S index, b value, energy counts, decay counts, rise time, and peak amplitude. How to quantify the sensitivity of these indicators to rockburst warning needs further study. Source parameter warning and spatial-temporal distribution warning in microseismic monitoring, as well as time-domain parameter warning and frequency-domain feature warning in acoustic emission are the main methods of rockburst warning. Regardless of the warning method, the warning time obtained through rockburst precursor characteristics is not always reliable.

This is related to the strong randomness of the rockburst, while specific rockburst intensity levels cannot be obtained. This makes it difficult to effectively implement graduated prevention and control at a later stage. The current field application is usually based on the energy release characteristics to estimate the rockburst intensity level, which increases the bias caused by individual subjectivity. In the future, we should pay attention to the issue of rockburst warning time, and at the same time consider combining it with related intelligent devices to further study how to determine the rockburst intensity level more objectively through the trend of dynamic parameters such as energy release characteristics. In short, the development of a rockburst disaster whole process recording equipment to assist the site monitoring will greatly improve construction efficiency and safety.

Both microseismic monitoring and acoustic emission monitoring by receiving elastic wave signals. However, the difference is that microseismic monitoring is non-contact monitoring by monitoring and analyzing the seismic waves released by microseismic events to understand the state of underground rocks or geological structures. Acoustic emission is to understand the deformation, rupture or stress release of rocks or structures by monitoring and analyzing the tiny acoustic waves generated inside them, which belongs to contact monitoring. This determines that microseismic monitoring has a wider range and can monitor the location and energy of rockbursts in real time. On the contrary, in acoustic emission monitoring, although the positioning accuracy is higher, the monitoring range is much smaller, resulting in less satisfactory results when applied individually to practical engineering. Based on the characteristics of microseismic monitoring and acoustic emission monitoring, early warning relying only on certain indicators or a certain method of each is not comprehensive. Therefore, in the future, the joint early warning technology of multi-methods and multi-indicators should be further established and enriched. In addition, due to the large number of dynamic indicators and strong correlation, which combinations of indicators can be more effective for rockburst early warning needs to be further studied.

Machine learning methods have shown good predictive ability in comprehensive multi-indicator prediction, and they can effectively deal with the problem of non-linear relationships between multiple indicators. Therefore, it has been widely used in recent years. In terms of input data, the static input indicators of the machine learning methods focus on maximum tangential stress σ_θ , compressive strength σ_c , tensile strength σ_t , brittleness index σ_c/σ_t , Stresscoefficient σ_θ/σ_c and elastic energy index W_{et} , Dynamic input indicators focus on Microseismic energy, seismic moment, cumulative event count, cumulative apparent volume and apparent stress. Although the above indicators are representative, they cannot cover the effects of tunnel depth and stress drop on rockburst. In general, the more input indicators, the better the model classification effect, so the future should be combined with more indicators to improve the rockburst prediction ability. For example, combining MS raw wave data and parametric data can significantly improve the prediction performance (Ji et al. 2020). In addition, the high prediction accuracy of current machine learning methods is still dominated by small sample datasets. For machine learning methods, small sample datasets limit the prediction performance of machine learning methods to a certain extent. Therefore, the establishment of larger databases in the future is necessary to improve the prediction performance.

It is worth noting that rockburst data have a family resemblance structure, which may affect the original nature of the data indicators when processing the data. For example, the elimination and replacement of outliers may destroy the original characteristics of the indicators, leading to a reduction in the objectivity of the data. Therefore, how to minimize the damage to the original rockburst data and how to quantify the degree of impact on the

rockburst prediction of the change in the original characteristics of the indicators after data processing needs to be considered by scholars.

At the level of algorithmic structure, traditional shallow machine learning methods generally suffer from catastrophic forgetting. One of the main reasons is that a large number of algorithmic models assume that the data distribution is steady and the samples are independently and identically distributed, so that the algorithmic models can repeatedly learn data with the same constructive features. There are unsteady data distributions in static and dynamic data, such as microseismic raw signal waveform data, which are not only unsteady but also a continuous data stream. Incremental learning in deep learning can effectively solve the catastrophic forgetting problem. However, there are not many incremental learning algorithms used for rockburst prediction, so further research on incremental learning should be carried out in the future to broaden its scope of application in the field of rockburst prediction.

Ensemble learning synthesizes multiple basic classifiers, and its prediction performance is better than that of a single basic classifier. Currently, ensemble learning uses either static or dynamic indicators as input indicators to the integrated model. In the future, is it possible to consider establishing hybrid indicators based on static and dynamic indicators? Its feasibility needs further research.

7 Conclusions

This paper presents a systematic review of rockburst prediction methods based on static and dynamic indicators from the nature of indicators. First, the importance analysis of rockburst prediction methods was conducted based on Citespace software. The results show that microseismic monitoring, acoustic emission, and machine learning have the highest degree of importance. Through the scientometric analysis, the rockburst prediction methods were focused on four methods: empirical methods, microseismic monitoring, acoustic emission, and machine learning. Then, the application of the four prediction methods is analyzed and summarized from the perspective of static and dynamic indexes, and the following conclusions are obtained:

- (1) The stress method's parameters are static quantitative indicators, while the energy method's parameters consider the dynamic behavior of the rock system. The latter method, based on energy indicators, better reflects the tendency of rockburst and has a more accurate prediction effect. The comprehensive index evaluation method can predict a variety of static indicators jointly, with energy feedback stress characteristics, showing better prediction performance than single-indicator methods. In the future, research should focus on the non-uniformity of the criterion formula and the problem of non-uniformity of the grading interval.
- (2) Microseismic monitoring has a main defect in that it has a prediction delay effect and cannot predict the specific time and intensity level of rockburst occurrences. The accuracy and validity of spatio-temporal distribution of characteristic cloud maps are significantly affected by MS signal processing. The introduction of artificial intelligence technology into MS signal processing is a future trend.
- (3) Acoustic emission monitoring techniques developed for indoor testing have not yet been applied in the engineering field. Further research is needed to determine how to transition from indoor testing to field monitoring. Although prediction miscalculation and

- prediction hysteresis have less influence on the time domain waveform warning, they remain a key research topic. The integration of time domain parameters and waveform characteristics into early warning methods is expected to become a mainstream trend.
- (4) Machine learning methods for indicators face several challenges, including missing data, unbalanced datasets, anomalous data values, indicator dependency, indicator assignment, and small sample databases. To minimize damage to the original features of the indicator data, the focus should be on data processing. Further research on advanced algorithmic structures to increase the intensity of data processing and expand the database is key to solving these problems.

No matter which prediction method, it has its advantages and shortcomings, no one method can be used to predict the rockburst activity of all projects. The key to the selection of the best model for rockburst prediction lies in the accuracy and applicability of static and dynamic indicators.

Author contributions All authors contributed to the study's conception and design. The first draft of the manuscript was written by Qinghe Zhang. Material preparation, data collection, and analysis were performed by Weiguo Li, Liang Yuan, Tianle Zheng, Zhiwei Liang, and Xiaorui Wang. All authors commented on previous versions of the manuscript. All authors read and approved the final manuscript.

Funding This work was supported by the National Engineering Research Centre Open Project (EC2022011), the National Major Research Instrument Development Project (52227901), the Anhui Provincial Universities Outstanding Young Research Funding Project (2022AH030088), the Anhui Provincial Universities Collaborative Innovation Funding Project (GXXT-2022-020).

Declarations

Conflict of interest The authors declare that they have no known competing financial interests or personal relationships that could have appeared to influence the work reported in this paper.

References

- Adoko AC, Gokceoglu C, Wu L, Zuo QJ (2013) Knowledge-based and data-driven fuzzy modeling for rockburst prediction. *Int J Rock Mech Min Sci* 61:86–95. <https://doi.org/10.1016/j.ijrmms.2013.02.010>
- Afraei S, Shahriar K, Madani SH (2019) Developing intelligent classification models for rock burst prediction after recognizing significant predictor variables, section: Literature review and data preprocessing procedure. *Tunn Undergr Space Technol* 83:324–353
- Ban YX, Fu X, Xie Q (2020) Revealing the laminar shale microdamage mechanism considering the relationship between fracture geometrical morphology and acoustic emission power spectrum characteristics. *Bull Eng Geol Environ* 79(2):1083–1096. <https://doi.org/10.1007/s10064-019-01599-8>
- Barton N, Lien R, Lunde J (1974) Engineering classification of rock masses for the design of tunnel support. *Rock Mech* 6:189–236
- Becker D, Cailleau B, Dahm T, Shapiro S, Kaiser D (2010) Stress triggering and stress memory observed from acoustic emission records in a salt mine. *Geophys J Int* 182(2):933–948. <https://doi.org/10.1111/j.1365-246X.2010.04642.x>
- Browning J, Meredith PG, Stuart CE, Healy D, Harland S, Mitchell TM (2017) Acoustic characterization of crack damage evolution in sandstone deformed under conventional and true triaxial loading. *J Geophys Res-Solid Earth* 122(6):4395–4412. <https://doi.org/10.1002/2016jb013646>
- Bukowska M (2012) The rockbursts in the upper silesian coal basin in Poland. *J Min Sci* 48:445–456
- Cai MF (2016) Prediction and prevention of rockburst in metal mines—a case study of Sanshandao gold mine. *J Rock Mech Geotech Eng* 8(2):204–211. <https://doi.org/10.1016/j.jrmge.2015.11.002>

- Cai W, Dou LM, Gong SY, Li ZL, Yuan SS (2014) Quantitative analysis of seismic velocity tomography in rock burst hazard assessment. *Nat Hazards* 75(3):2453–2465. <https://doi.org/10.1007/s11069-014-1443-6>
- Castro L, Bewick R, Carter T (2012) An overview of numerical modelling applied to deep mining. *Innovative numerical modelling in geomechanics*. CRC Press, pp 393–414
- Chai MY, Zhang ZX, Duan Q (2018) A new qualitative acoustic emission parameter based on Shannon's entropy for damage monitoring. *Mech Syst Signal Proc* 100:617–629. <https://doi.org/10.1016/j.ymssp.2017.08.007>
- Chen BR, Wu H, Chi XW, Liu H, Wu MD, Yan JW (2019) Real-time recognition algorithm for microseismic signals of rock failure based on STA/LTA and its engineering application. *Rock Soil Mech* 40(9):3689–3696. <https://doi.org/10.16285/j.rsm.2018.1017>
- Cheng WC, Li G, Liu NN, Xu J, Horpibulsuk S (2020) Recent massive incidents for subway construction in soft alluvial deposits of Taiwan: a review. *Tunn Undergr Space Technol* 96:18. <https://doi.org/10.1016/j.tust.2019.103178>
- Cui X, Wong LNY (2023) Extensive propagation of 3D wing cracks under compression. *Rock Mech Rock Eng*. <https://doi.org/10.1007/s00603-023-03358-4>
- Dai LP, Pan YS, Zhang CG, Wang AW, Canbulat I, Shi TW, Wei CC, Cai RH, Liu FY, Gao XP (2022) New criterion of critical mining stress index for risk evaluation of roadway rockburst. *Rock Mech Rock Eng* 55(8):4783–4799. <https://doi.org/10.1007/s00603-022-02888-7>
- Deng L, Wu J, Lv Y (2012) Study on rockburst energy index method based on the rock stress-strain curve. *Railw Stand Des* 7:108–111. <https://doi.org/10.13238/j.issn.1004-2954.2012.07.002>
- Di YY, Wang EY (2021) Rock burst precursor electromagnetic radiation signal recognition method and early warning application based on recurrent neural networks. *Rock Mech Rock Eng* 54(3):1449–1461. <https://doi.org/10.1007/s00603-020-02314-w>
- Ding ZW, Li XF, Tang QB, Jia JD, Gao CD, Wang SY, Wang SF (2022) Research on rock crack classification based on acoustic emission waveform feature extraction technology. *Lithosphere*. <https://doi.org/10.2113/2022/5804064>
- Dong LJ, Li XB, Peng K (2013) Prediction of rockburst classification using random forest. *Trans Nonferrous Metal Soc* 23(2):472–477. [https://doi.org/10.1016/s1003-6326\(13\)62487-5](https://doi.org/10.1016/s1003-6326(13)62487-5)
- Dong LJ, Zhang LY, Liu HN, Du K, Liu XL (2022) Acoustic emission b value characteristics of granite under true triaxial stress. *Mathematics*. <https://doi.org/10.3390/math10030451>
- Dou LM, Cai W, Cao AY, Guo WH (2018) Comprehensive early warning of rock burst utilizing microseismic multi-parameter indices. *Int J Min Sci Technol* 28(5):767–774. <https://doi.org/10.1016/j.ijmst.2018.08.007>
- Du JS, Chen J, Pu YY, Jiang DY, Chen LL, Zhang YR (2021) Risk assessment of dynamic disasters in deep coal mines based on multi-source, multi-parameter indexes, and engineering application. *Process Saf Environ* 155:575–586. <https://doi.org/10.1016/j.psep.2021.09.034>
- Du CL, Pan YC, Liu QS, Huang X, Yin X (2022) Rockburst inoculation process at different structural planes and microseismic warning technology: a case study. *Bull Eng Geol Environ* 81(12):499
- Faradonbeh RS, Haghshenas SS, Taheri A, Mikael R (2020) Application of self-organizing map and fuzzy c-mean techniques for rockburst clustering in deep underground projects. *Neural Comput Appl* 32(12):8545–8559. <https://doi.org/10.1007/s00521-019-04353-z>
- Feng XT, Wang LN (1994) Rockburst prediction based on neural networks. *Trans Nonferrous Metal Soc* 4(1):7–14
- Feng GL, Feng XT, Chen BR, Xiao YX, Yu Y (2015) A microseismic method for dynamic warning of rockburst development processes in tunnels. *Rock Mech Rock Eng* 48(5):2061–2076. <https://doi.org/10.1007/s00603-014-0689-3>
- Feng GL, Xia GQ, Chen BR, Xiao YX, Zhou RC (2019) A method for rockburst prediction in the deep tunnels of hydropower stations based on the monitored microseismicity and an optimized probabilistic neural network model. *Sustainability*. <https://doi.org/10.3390/su11113212>
- Fu L, Mao SD, Chen F, Zhao SC, Su WT, Lai GS, Yu AM, Lin CT (2022) Graphene-based electrochemical sensors for antibiotic detection in water, food and soil: a scientometric analysis in CiteSpace (2011–2021). *Chemosphere* 297:14. <https://doi.org/10.1016/j.chemosphere.2022.134127>
- Gao L, Gao F, Xing Y, Zhang ZZ (2020) An energy preservation index for evaluating the rockburst potential based on energy evolution. *Energies*. <https://doi.org/10.3390/en13143636>
- Gao L, Liu ZK, Zhang HY (2021) Prediction of rockburst classification of railway tunnel based on hybrid PSO-RBF neural network. *J Railw Sci Eng* 18(2):450–458
- Gao AS, Qi CZ, Shan RL, Wang CL, Kocharyan GG (2023) Identification and early warning method of key disaster-causing factors of AE signals for red sandstone by principal component analysis method. *Ain Shams Eng J*. <https://doi.org/10.1016/j.asej.2023.102205>

- Ghasemi E, Gholizadeh H, Adoko AC (2019) Evaluation of rockburst occurrence and intensity in underground structures using decision tree approach. *Eng Comput* 36(1):213–225. <https://doi.org/10.1007/s00366-018-00695-9>
- Gnip P, Vokorokos L, Drotar P (2021) Selective oversampling approach for strongly imbalanced data. *PeerJ Comput Sci*. <https://doi.org/10.7717/peerj-cs.604>
- Gong F, Li X (2007) A distance discriminant analysis method for prediction of possibility and classification of rockburst and its application. *Chin J Rock Mech Eng* 26(5):1012–1018
- Gong QM, Yin LJ, Wu SY, Zhao J, Ting Y (2012) Rock burst and slabbing failure and its influence on TBM excavation at headrace tunnels in Jinping II hydropower station. *Eng Geol* 124:98–108. <https://doi.org/10.1016/j.enggeo.2011.10.007>
- Gong F, Yan J, Li X (2018a) A new criterion of rock burst proneness based on the linear energy storage law and the residual elastic energy index. *Chin J Rock Mech Eng* 37(9):1993–2014
- Gong FQ, Yan JY, Li XB (2018b) A new criterion of rock burst proneness based on the linear energy storage law and the residual elastic energy index. *Chin J Rock Mech Eng* 37(9):1993–2014. <https://doi.org/10.13722/j.cnki.jrme.2018.0232>
- Gong FQ, Yan JY, Li XB, Luo S (2019) A peak-strength strain energy storage index for rock burst proneness of rock materials. *Int J Rock Mech Min Sci* 117:76–89. <https://doi.org/10.1016/j.ijrmm.2019.03.020>
- Gong FQ, Wang YL, Luo S (2020) Rockburst proneness criteria for rock materials: review and new insights. *J Cent South Univ* 27(10):2793–2821. <https://doi.org/10.1007/s11771-020-4511-y>
- Gong FQ, Wang YL, Wang ZG, Pan JF, Luo S (2021) A new criterion of coal burst proneness based on the residual elastic energy index. *Int J Min Sci Technol* 31(4):553–563. <https://doi.org/10.1016/j.ijmst.2021.04.001>
- Guo C, Zhu TY, Gao YT, Wu SC, Sun J (2021a) AEnet: automatic picking of p-wave first arrivals using deep learning. *IEEE Trans Geosci Remote Sens* 59(6):5293–5303. <https://doi.org/10.1109/tgrs.2020.3010541>
- Guo DP, Chen HM, Tang LB, Chen ZX, Samui P (2021b) Assessment of rockburst risk using multivariate adaptive regression splines and deep forest model. *Acta Geotech* 17(4):1183–1205. <https://doi.org/10.1007/s11440-021-01299-2>
- Guo J, Guo JW, Zhang QL, Huang MJ (2022) Research on rockburst classification prediction based on BP-SVM model. *IEEE Access* 10:50427–50447. <https://doi.org/10.1109/access.2022.3173059>
- Hao JW, Qiao L, Li ZJ, Li QW (2022) Analysis on rock fracture signals and exploration of infrared advance prediction under true triaxial loading. *J Mater Civ Eng*. [https://doi.org/10.1061/\(asce\)mt.1943-5533.0004202](https://doi.org/10.1061/(asce)mt.1943-5533.0004202)
- He YY, Zheng YY (2018) Short-term power load probability density forecasting based on Yeo-Johnson transformation quantile regression and Gaussian kernel function. *Energy* 154:143–156. <https://doi.org/10.1016/j.energy.2018.04.072>
- He MC, Sousa LRE, Miranda T, Zhu GL (2015) Rockburst laboratory tests database-application of data mining techniques. *Eng Geol* 185:116–130. <https://doi.org/10.1016/j.enggeo.2014.12.008>
- He MM, Zhang ZQ, Zheng J, Chen FF, Li N (2020) A new perspective on the constant m of the Hoek-Brown failure criterion and a new model for determining the residual strength of rock. *Rock Mech Rock Eng* 53(9):3953–3967. <https://doi.org/10.1007/s00603-020-02164-6>
- He SY, Lai JX, Zhong YJ, Wang K, Xu W, Wang LX, Liu T, Zhang CP (2021) Damage behaviors, prediction methods and prevention methods of rockburst in 13 deep traffic tunnels in China. *Eng Fail Anal*. <https://doi.org/10.1016/j.engfailanal.2020.105178>
- He MC, Cheng T, Qiao YF, Li HR (2023) A review of rockburst: experiments, theories, and simulations. *J Rock Mech Geotech Eng* 15(5):1312–1353. <https://doi.org/10.1016/j.jrmge.2022.07.014>
- Hoek E, Brown E (1980) *Underground excavations in rock*. CRC Press, London
- Hoek E, Brown ET (1997) Practical estimates of rock mass strength. *Int J Rock Mech Min Sci* 34(8):1165–1186
- Hosseini Z, Beruar O, Sampson-Forsythe A, Yao M (2010) Mining strategies of multi-sill pillars in burst prone ground conditions at vale inco's coleman mine. In: 44th US Rock Mechanics Symposium and 5th US-Canada Rock Mechanics Symposium. OnePetro.
- Hu XC, Su GS, Chen GY, Mei SM, Feng XT, Mei GX, Huang XH (2018) Experiment on rockburst process of borehole and its acoustic emission characteristics. *Rock Mech Rock Eng* 52(3):783–802. <https://doi.org/10.1007/s00603-018-1613-z>
- Iqbal N, Zerguine A, Kaka S, Al-Shuhail A (2018) Observation-driven method based on IIR Wiener filter for microseismic data denoising. *Pure Appl Geophys* 175(6):2057–2075. <https://doi.org/10.1007/s00024-018-1775-3>

- Ji B, Xie F, Wang XP, He SQ, Song DZ (2020) Investigate contribution of multi-microseismic data to rockburst risk prediction using support vector machine with genetic algorithm. *IEEE Access* 8:58817–58828. <https://doi.org/10.1109/access.2020.2982366>
- Jiang Q, Su GS, Feng XT, Chen GQ, Zhang MZ, Liu C (2019) Excavation optimization and stability analysis for large underground caverns under high geostress: A case study of the Chinese Laxiwa project. *Rock Mech Rock Eng* 52(3):895–915. <https://doi.org/10.1007/s00603-018-1605-z>
- Jiang JQ, Su GS, Yan ZF, Zheng Z, Hu XC (2022) Rock crack type identification by Gaussian process learning on acoustic emission. *Appl Acoust*. <https://doi.org/10.1016/j.apacoust.2022.108926>
- Jin XC, Zhou ZH (2012) Energy formula of rockburst. *Metal Mine* 434(8):40–43
- Jin AB, Basnet PMS, Mahtab S (2022) Microseismicity-based short-term rockburst prediction using non-linear support vector machine. *Acta Geophys* 70(4):1717–1736. <https://doi.org/10.1007/s11600-022-00817-4>
- Kaiser PK, Cai M (2012) Design of rock support system under rockburst condition. *J Rock Mech Geotech Eng* 4(3):215–227
- Kaiser PK, Tannant DD, McCreath DR (1996) Drift support in burst-prone ground. *CIM Bull* 89(998):131–138
- Kamran M, Ullah B, Ahmad M, Sabri MMS (2022) Application of KNN-based isometric mapping and fuzzy c-means algorithm to predict short-term rockburst risk in deep underground projects. *Front Public Health* 10:1023890. <https://doi.org/10.3389/fpubh.2022.1023890>
- Ke B, Khandelwal M, Asteris PG, Skentou AD, Mamou A, Armaghani DJ (2021) Rock-burst occurrence prediction based on optimized Naïve Bayes models. *IEEE Access* 9:91347–91360. <https://doi.org/10.1109/access.2021.3089205>
- Keneti A, Sainsbury BA (2018) Review of published rockburst events and their contributing factors. *Eng Geol* 246:361–373. <https://doi.org/10.1016/j.enggeo.2018.10.005>
- Khan NM, Ahmad M, Cao KW, Ali I, Liu W, Rehman H, Hussain S, Rehman FU, Ahmed T (2022) Developing a new bursting liability index based on energy evolution for coal under different loading rates. *Sustainability*. <https://doi.org/10.3390/su14031572>
- Khan M, He XQ, Song DZ, Tian XH, Li ZL, Xue YR, Aslam KS (2023) Extracting and predicting rock mechanical behavior based on microseismic spatio-temporal response in an ultra-thick coal seam mine. *Rock Mech Rock Eng* 56(5):3725–3754. <https://doi.org/10.1007/s00603-023-03247-w>
- Kidybiński A (1981) Bursting liability indices of coal. *Int J Rock Mech Min Sci Geomech Abstr* 18:295–304
- Kiyoo M (1962) Study of elastic shocks caused by the fracture of heterogeneous materials and its relations to earthquake phenomena. *Bull Earthq Res Inst Univ Tokyo* 40:125–173
- Li N, Jimenez R (2017) A logistic regression classifier for long-term probabilistic prediction of rock burst hazard. *Nat Hazards* 90(1):197–215. <https://doi.org/10.1007/s11069-017-3044-7>
- Li T, Cai MF, Cai M (2007) A review of mining-induced seismicity in China. *Int J Rock Mech Min Sci* 44(8):1149–1171. <https://doi.org/10.1016/j.ijrmms.2007.06.002>
- Li LR, Deng JH, Zheng L, Liu JF (2017a) Dominant frequency characteristics of acoustic emissions in white marble during direct tensile tests. *Rock Mech Rock Eng* 50(5):1337–1346. <https://doi.org/10.1007/s00603-016-1162-2>
- Li N, Feng XD, Jimenez R (2017b) Predicting rock burst hazard with incomplete data using Bayesian networks. *Tunn Undergr Space Technol* 61:61–70. <https://doi.org/10.1016/j.tust.2016.09.010>
- Li TZ, Li YX, Yang XL (2017c) Rock burst prediction based on genetic algorithms and extreme learning machine. *J Cent South Univ* 24(9):2105–2113. <https://doi.org/10.1007/s11771-017-3619-1>
- Li CC, Mikula P, Simser B, Hebblewhite B, Joughin W, Feng XW, Xu NW (2019) Discussions on rockburst and dynamic ground support in deep mines. *J Rock Mech Geotech Eng* 11(5):1110–1118
- Li X, Mao HY, Li B, Xu NW (2021) Dynamic early warning of rockburst using microseismic multi-parameters based on Bayesian network. *Eng Sci Technol Int J* 24(3):715–727. <https://doi.org/10.1016/j.jestch.2020.10.002>
- Li DY, Liu ZD, Armaghani DJ, Xiao P, Zhou J (2022a) Novel ensemble tree solution for rockburst prediction using deep forest. *Mathematics*. <https://doi.org/10.3390/math10050787>
- Li DY, Liu ZD, Xiao P, Zhou J, Jahed Armaghani D (2022b) Intelligent rockburst prediction model with sample category balance using feedforward neural network and Bayesian optimization. *Undergr Space* 7(5):833–846. <https://doi.org/10.1016/j.undsp.2021.12.009>
- Li GK, Xue YG, Qu CQ, Qiu DH, Wang P, Liu QS (2023a) Intelligent prediction of rockburst in tunnels based on back propagation neural network integrated beetle antennae search algorithm. *Environ Sci Pollut Res* 30(12):33960–33973. <https://doi.org/10.1007/s11356-022-24420-8>
- Li JY, Liu DQ, He MC, Guo YP (2023b) True triaxial experimental study on the variation characteristics of rockburst with the number of fast unloading surfaces. *Rock Mech Rock Eng*. <https://doi.org/10.1007/s00603-023-03311-5>

- Li ML, Li KG, Qin QC (2023c) A rockburst prediction model based on extreme learning machine with improved Harris Hawks optimization and its application. *Tunn Undergr Space Technol*. <https://doi.org/10.1016/j.tust.2022.104978>
- Li ML, Li KG, Qin QC, Yue R, Shi J (2023d) Research and application of an intelligent prediction of rock bursts based on a bayes-optimized convolutional neural network. *Int J Geomech*. <https://doi.org/10.1061/jgnai.Gmeng-8213>
- Liang WZ, Dai B, Zhao GY, Wu H (2020a) A scientometric review on rockburst in hard rock: two decades of review from 2000 to 2019. *Geofluids* 2020:1–17. <https://doi.org/10.1155/2020/8763283>
- Liang WZ, Sari A, Zhao GY, McKinnon SD, Wu H (2020b) Short-term rockburst risk prediction using ensemble learning methods. *Nat Hazards* 104(2):1923–1946. <https://doi.org/10.1007/s11069-020-04255-7>
- Liang ZZ, Xue RX, Xu NW, Li WR (2020c) Characterizing rockbursts and analysis on frequency-spectrum evolutionary law of rockburst precursor based on microseismic monitoring. *Tunn Undergr Space Technol*. <https://doi.org/10.1016/j.tust.2020.103564>
- Liang WZ, Sari YA, Zhao GY, McKinnon SD, Wu H (2021) Probability estimates of short-term rockburst risk with ensemble classifiers. *Rock Mech Rock Eng* 54(4):1799–1814. <https://doi.org/10.1007/s00603-021-02369-3>
- Liu ZD, Li DY (2023) Intelligent hybrid model to classify failure modes of overstressed rock masses in deep engineering. *J Cent South Univ* 30(1):156–174. <https://doi.org/10.1007/s11771-022-5208-1>
- Liu ZB, Shao JF, Xu WY, Meng YD (2013) Prediction of rock burst classification using the technique of cloud models with attribution weight. *Nat Hazards* 68(2):549–568. <https://doi.org/10.1007/s11069-013-0635-9>
- Liu F, Tang C, Ma TH, Tang LX (2019) Characterizing rockbursts along a structural plane in a tunnel of the Hanjiang-to-Weihe river diversion project by microseismic monitoring. *Rock Mech Rock Eng* 52(6):1835–1856. <https://doi.org/10.1007/s00603-018-1649-0>
- Liu CY, Du LZ, Zhang XP, Wang Y, Hu XM, Han YL (2021a) A new rock brittleness evaluation method based on the complete stress-strain curve. *Lithosphere* 2021:14. <https://doi.org/10.2113/2021/4029886>
- Liu GF, Jiang Q, Feng GL, Chen DF, Chen BR, Zhao ZN (2021b) Microseismicity-based method for the dynamic estimation of the potential rockburst scale during tunnel excavation. *Bull Eng Geol Environ* 80(5):3605–3628. <https://doi.org/10.1007/s10064-021-02173-x>
- Liu XQ, Xia YY, Lin MQ, Wang G, Wang DX (2021c) Experimental study on the influence of tangential stress gradient on the energy evolution of strainburst. *Bull Eng Geol Environ* 80(6):4515–4528. <https://doi.org/10.1007/s10064-021-02244-z>
- Liu HY, Zhang BY, Li XL, Liu CW, Wang C, Wang F, Chen DY (2022) Research on roof damage mechanism and control technology of gob-side entry retaining under close distance gob. *Eng Fail Anal*. <https://doi.org/10.1016/j.engfailanal.2022.106331>
- Liu HX, Zhao GY, Xiao P, Yin YT (2023a) Ensemble tree model for long-term rockburst prediction in incomplete datasets. *Minerals* 13(1):18. <https://doi.org/10.3390/min13010103>
- Liu W, Ma LQ, Gao QQ, Spearing AJS, Wang YY, Cui RY, Zhao ZY (2023b) Fracture precursor recognition and damage quantitative characterization of stressed rock using infrared radiation. *Rock Mech Rock Eng*. <https://doi.org/10.1007/s00603-023-03344-w>
- Liu XQ, Wang G, Song LB, Han GS, Chen WZ, Chen H (2023c) A new rockburst criterion of stress-strength ratio considering stress distribution of surrounding rock. *Bull Eng Geol Environ* 82(1):13. <https://doi.org/10.1007/s10064-022-03042-x>
- Luo S, Yan P, Lu WB, Dong ZH, Zhou CH, Yang ZW, Hu YG (2023) Stability index of surrounding rock during deep rock excavation considering energy release speed. *Appl Sci*. <https://doi.org/10.3390/app13053000>
- Ma K, Tang CA, Wang LX, Tang DH, Zhuang DY, Zhang QB, Zhao J (2016) Stability analysis of underground oil storage caverns by an integrated numerical and microseismic monitoring approach. *Tunn Undergr Space Technol* 54:81–91. <https://doi.org/10.1016/j.tust.2016.01.024>
- Ma TH, Tang CA, Tang SB, Kuang L, Yu Q, Kong DQ, Zhu X (2018) Rockburst mechanism and prediction based on microseismic monitoring. *Int J Rock Mech Min Sci* 110:177–188
- Ma CC, Li TB, Zhang H (2020) Microseismic and precursor analysis of high-stress hazards in tunnels: a case comparison of rockburst and fall of ground. *Eng Geol* 265:11. <https://doi.org/10.1016/j.enggeo.2019.105435>
- Ma K, Sun XY, Zhang ZH, Hu J, Wang ZR (2022a) Intelligent location of microseismic events based on a fully convolutional neural network (FCNN). *Rock Mech Rock Eng* 55(8):4801–4817. <https://doi.org/10.1007/s00603-022-02911-x>

- Ma TH, Lin DY, Tang LX, Li LM, Tang CN, Yadav KP, Jin WD (2022b) Characteristics of rockburst and early warning of microseismic monitoring at qinling water tunnel. *Geomat Nat Hazards Risk* 13(1):1366–1394. <https://doi.org/10.1080/19475705.2022.2073830>
- Ma K, Shen QQ, Sun XY, Ma TH, Hu J, Tang CA (2023) Rockburst prediction model using machine learning based on microseismic parameters of Qinling water conveyance tunnel. *J Cent South Univ* 30(1):289–305. <https://doi.org/10.1007/s11771-023-5233-8>
- Marsland S (2015) *Machine learning: an algorithmic perspective*. CRC Press
- Mei FD, Hu CY, Li PY, Zhang JS (2019) Study on main frequency precursor characteristics of acoustic emission from deep buried dali rock explosion. *Arab J Geosci*. <https://doi.org/10.1007/s12517-019-4706-4>
- Meng FZ, Zhou H, Li SJ, Zhang CQ, Wang ZQ, Kong L, Zhang LM (2016) Shear behaviour and acoustic emission characteristics of different joints under various stress levels. *Rock Mech Rock Eng* 49(12):4919–4928. <https://doi.org/10.1007/s00603-016-1034-9>
- Meng FZ, Zhou H, Wang ZQ, Zhang LM, Kong L, Li SJ, Zhang CQ, Hu SC (2017) Experimental study of factors affecting fault slip rockbursts in deeply buried hard rock tunnels. *Bull Eng Geol Environ* 76:1167–1182
- Mogamedi KA, Stacey TR (2019) Value creation as an approach to the management and control of rockburst damage in tunnels. *Tunn Undergr Space Technol* 83:545–551. <https://doi.org/10.1016/j.tust.2018.08.023>
- Morgenroth J, Perras MA, Khan UT (2022) A convolutional neural network approach for predicting tunnel liner yield at cigar lake mine. *Rock Mech Rock Eng* 55(5):2821–2843. <https://doi.org/10.1007/s00603-021-02563-3>
- Mousavi SM, Langston CA (2016) Adaptive noise estimation and suppression for improving microseismic event detection. *J Appl Geophys* 132:116–124. <https://doi.org/10.1016/j.jappgeo.2016.06.008>
- Pan PZ, Miao ST, Wu ZH, Feng XT, Shao CY (2020) Laboratory observation of spalling process induced by tangential stress concentration in hard rock tunnel. *Int J Geomech* 20(3):15. [https://doi.org/10.1061/\(asce\)gm.1943-5622.0001620](https://doi.org/10.1061/(asce)gm.1943-5622.0001620)
- Peng GL, Tuo XG, Shen T, Lu J (2021) Recognition of rock micro-fracture signal based on deep convolution neural network inception algorithm. *IEEE Access* 9:89390–89399. <https://doi.org/10.1109/access.2021.3086630>
- Pu YY, Apel DB, Wang C, Wilson B (2018) Evaluation of burst liability in kimberlite using support vector machine. *Acta Geophys* 66(5):973–982. <https://doi.org/10.1007/s11600-018-0178-2>
- Pu YY, Apel DB, Liu V, Mitri H (2019a) Machine learning methods for rockburst prediction-state-of-the-art review. *Int J Min Sci Technol* 29(4):565–570. <https://doi.org/10.1016/j.ijmst.2019.06.009>
- Pu YY, Apel DB, Xu HW (2019b) Rockburst prediction in kimberlite with unsupervised learning method and support vector classifier. *Tunn Undergr Space Technol* 90:12–18. <https://doi.org/10.1016/j.tust.2019.04.019>
- Pu YY, Apel DB, Hall R (2020) Using machine learning approach for microseismic events recognition in underground excavations: comparison of ten frequently-used models. *Eng Geol* 268:13. <https://doi.org/10.1016/j.enggeo.2020.105519>
- Qu HL, Yang LH, Zhu JB, Chen S, Li BW, Li B (2022) A multi-index evaluation method for rockburst proneness of deep underground rock openings with attribute recognition model and its application. *Int J Rock Mech Min Sci*. <https://doi.org/10.1016/j.ijrmms.2022.105225>
- Rabinovitch A, Bahat D, Frid V (2002) Similarity and dissimilarity of electromagnetic radiation from carbonate rocks under compression, drilling and blasting. *Int J Rock Mech Min Sci* 39(1):125–129
- Ren FQ, Zhu C, He MC, Shang JL, Feng GL, Bai JW (2023) Characteristics and precursor of static and dynamic triggered rockburst: insight from multifractal. *Rock Mech Rock Eng* 56(3):1945–1967. <https://doi.org/10.1007/s00603-022-03173-3>
- Rusnes B (1974) Analysis of rock spalling for tunnels in steep valley sides. Norwegian Institute of Technology
- Sagi O, Rokach L (2018) Ensemble learning: a survey. *Wiley Interdiscip Rev-Data Min Knowl Discov* 8(4):18. <https://doi.org/10.1002/widm.1249>
- Shang YJ, Zhang JJ, Fu BJ (2013) Analyses of three parameters for strain mode rockburst and expression of rockburst potential. *Chin J Rock Mech Eng* 32(8):1520–1527
- Shirani Faradonbeh R, Taheri A, Ribeiro e Sousa L, Karakus M (2020) Rockburst assessment in deep geo-technical conditions using true-triaxial tests and data-driven approaches. *Int J Rock Mech Min Sci*. <https://doi.org/10.1016/j.ijrmms.2020.104279>
- Shukla R, Khandelwal M, Kankar PK (2021) Prediction and assessment of rock burst using various meta-heuristic approaches. *Mining Metall Explor* 38(3):1375–1381. <https://doi.org/10.1007/s42461-021-00415-w>

- Qui SL, Feng XT, Jiang Q, Zhang CQ (2014) A novel numerical index for estimating strainburst vulnerability in deep tunnels. *Chin J Rock Mech Eng* 33(10):2007–2017. <https://doi.org/10.13722/j.cnki.jrme.2014.10.007>
- Song GD, Cheng JL, Grattan KTV (2020) Recognition of microseismic and blasting signals in mines based on convolutional neural network and stockwell transform. *IEEE Access* 8:45523–45530. <https://doi.org/10.1109/access.2020.2978392>
- Strawn GO (2022) Masterminds of deep learning. *IT Prof* 24(3):13–14. <https://doi.org/10.1109/mitp.2022.3172838>
- Su GS, Shi YJ, Feng XT, Jiang JQ, Zhang J, Jiang Q (2017) True-triaxial experimental study of the evolutionary features of the acoustic emissions and sounds of rockburst processes. *Rock Mech Rock Eng* 51(2):375–389. <https://doi.org/10.1007/s00603-017-1344-6>
- Su GS, Ren HY, Jiang JQ, Hu XC (2023) Experimental study on the characteristics of rockburst occurring at the working face during tunnel excavation. *Int J Rock Mech Min Sci* 164:16. <https://doi.org/10.1016/j.ijrmmms.2023.105347>
- Sun YT, Li GC, Yang S (2021a) Rockburst Interpretation by a data-driven approach: a comparative study. *Mathematics*. <https://doi.org/10.3390/math9222965>
- Sun YT, Li GC, Zhang JF, Huang JD (2021b) Rockburst intensity evaluation by a novel systematic and evolved approach: machine learning booster and application. *Bull Eng Geol Environ* 80(11):8385–8395. <https://doi.org/10.1007/s10064-021-02460-7>
- Sun LJ, Hu NY, Ye YC, Tan WK, Wu ML, Wang XH, Huang ZY (2022) Ensemble stacking rockburst prediction model based on Yeo-Johnson, K-means SMOTE, and optimal rockburst feature dimension determination. *Sci Rep* 12(1):15352. <https://doi.org/10.1038/s41598-022-19669-5>
- Tan YL, Ma Q, Liu XS, Zhao ZH, Zhao MX, Li L (2022) Failure prediction from crack evolution and acoustic emission characteristics of coal-rock sandwich composite samples under uniaxial compression. *Bull Eng Geol Environ*. <https://doi.org/10.1007/s10064-022-02705-z>
- Tang CA, Li LC, Xu NW, Ma K (2015) Microseismic monitoring and numerical simulation on the stability of high-steep rock slopes in hydropower engineering. *J Rock Mech Geotech Eng* 7(5):493–508. <https://doi.org/10.1016/j.jrmge.2015.06.010>
- Tang SB, Wang JX, Tang CN (2021) Identification of microseismic events in rock engineering by a convolutional neural network combined with an attention mechanism. *Rock Mech Rock Eng* 54(1):47–69. <https://doi.org/10.1007/s00603-020-02259-0>
- Tao M, Li ZW, Cao WZ, Li XB, Wu CQ (2019) Stress redistribution of dynamic loading incident with arbitrary waveform through a circular cavity. *Int J Numer Anal Methods Geomech* 43(6):1279–1299. <https://doi.org/10.1002/nag.2897>
- Tao ZY (1988) Support design of tunnels subjected to rockbursting. In: *ISRM International Symposium. OnePetro*.
- Tian J, Chen D, Liu Z, Sun W (2022) Microseismic dynamic response and multi-source warning during rockburst monitoring based on weight decision analysis. *Int J Environ Res Public Health*. <https://doi.org/10.3390/ijerph192315698>
- Turchaninov I, Markov G, Gzovsky M, Kazikayev D, Frenze U, Batugin S, Chabdarova U (1972) State of stress in the upper part of the Earth's crust based on direct measurements in mines and on tectonophysical and seismological studies. *Phys Earth Planet Inter* 6(4):229–234
- Van der Maaten L, Hinton G (2008) Visualizing data using t-SNE. *J Mach Learn Res* 9:2579–2605
- Wang EY, He XQ, Wei JP, Nie BS, Song DZ (2011) Electromagnetic emission graded warning model and its applications against coal rock dynamic collapses. *Int J Rock Mech Min Sci* 48(4):556–564. <https://doi.org/10.1016/j.ijrmmms.2011.02.006>
- Wang QW, Ju NP, Du LL, Huang J, Hu Y (2018a) Three dimensional inverse analysis of geostress field in the Sangri-Jiacha section of Lasa-Linzi railway. *Rock Soil Mech* 39(4):1450–1462
- Wang SF, Li XB, Wang SY (2018b) Three-dimensional mineral grade distribution modelling and long-wall mining of an underground bauxite seam. *Int J Rock Mech Min Sci* 103:123–136. <https://doi.org/10.1016/j.ijrmmms.2018.01.035>
- Wang SF, Li XB, Yao JR, Gong FQ, Li X, Du K, Tao M, Huang LQ, Du SL (2019) Experimental investigation of rock breakage by a conical pick and its application to non-explosive mechanized mining in deep hard rock. *Int J Rock Mech Min Sci* 122:14. <https://doi.org/10.1016/j.ijrmmms.2019.104063>
- Wang CB, Si GY, Zhang CG, Cao AY, Canbulat I (2021a) A statistical method to assess the data integrity and reliability of seismic monitoring systems in underground mines. *Rock Mech Rock Eng* 54(11):5885–5901. <https://doi.org/10.1007/s00603-021-02597-7>
- Wang CL, Cao C, Liu YB, Li CF, Li GY, Lu H (2021b) Experimental investigation on synergetic prediction of rockburst using the dominant-frequency entropy of acoustic emission. *Nat Hazards* 108(3):3253–3270. <https://doi.org/10.1007/s11069-021-04822-6>

- Wang HL, Li ZL, Song DZ, He XQ, Sobolev A, Khan M (2021c) An intelligent rockburst prediction model based on scorecard methodology. *Minerals*. <https://doi.org/10.3390/min1111294>
- Wang JB, Zhang Q, Song ZP, Zhang YW (2021d) Experimental study on creep properties of salt rock under long-period cyclic loading. *Int J Fatigue* 143:10. <https://doi.org/10.1016/j.ijfatigue.2020.106009>
- Wang YC, Tang CA, Tang LX, Zhang SC, Li LM, Li YB, Duan WS (2021e) Microseismicity characteristics before and after a rockburst and mechanisms of intermittent rockbursts in a water diversion tunnel. *Rock Mech Rock Eng* 55(1):341–361. <https://doi.org/10.1007/s00603-021-02666-x>
- Wang CL, Cao C, Li CF, Chuai XS, Zhao GM, Lu H (2022) Experimental investigation on synergetic prediction of granite rockburst using rock failure time and acoustic emission energy. *J Cent South Univ* 29(4):1262–1273. <https://doi.org/10.1007/s11771-022-4971-3>
- Wang KK, Ma K, Tang CA, Liu HY, Wang XT, Li Q (2023a) Study on deep mining-induced strata behavior based on the evolutionary laws of multiple indices from microseismic monitoring. *Rock Mech Rock Eng*. <https://doi.org/10.1007/s00603-023-03411-2>
- Wang YC, Tang CA, Cai M, Tang LX, Ma TH, Zhang SC, Li LM, Li YB (2023b) Microseismicity evolution related to two extremely intense rockbursts in a water diversion tunnel. *Int J Rock Mech Min Sci* 164:13. <https://doi.org/10.1016/j.ijrmmms.2023.105359>
- Wu SC, Wu ZG, Zhang CX (2019) Rock burst prediction probability model based on case analysis. *Tunn Undergr Space Technol*. <https://doi.org/10.1016/j.tust.2019.103069>
- Wu K, Shao ZS, Qin S, Wei W, Chu ZF (2021) A critical review on the performance of yielding supports in squeezing tunnels. *Tunn Undergr Space Technol* 115:21. <https://doi.org/10.1016/j.tust.2021.103815>
- Xiao FK, He J, Liu ZJ, Shen ZL, Liu G (2019) Analysis on warning signs of damage of coal samples with different water contents and relevant damage evolution based on acoustic emission and infrared characterization. *Infrared Phys Technol* 97:287–299. <https://doi.org/10.1016/j.infrared.2019.01.007>
- Xie XB, Li DX, Kong LY, Ye YF, Gao S (2020) Rockburst propensity prediction model based on CRITIC-XGB algorithm. *Chin J Rock Mech Eng* 39(10):1975–1982. <https://doi.org/10.13722/j.cnki.jrme.2019.1049>
- Xue RX, Liang ZZ, Xu NW, Dong LL (2020a) Rockburst prediction and stability analysis of the access tunnel in the main powerhouse of a hydropower station based on microseismic monitoring. *Int J Rock Mech Min Sci*. <https://doi.org/10.1016/j.ijrmmms.2019.104174>
- Xue YG, Bai CH, Qiu DH, Kong FM, Li ZQ (2020b) Predicting rockburst with database using particle swarm optimization and extreme learning machine. *Tunn Undergr Space Technol*. <https://doi.org/10.1016/j.tust.2020.103287>
- Xue RX, Liang ZZ, Xu NW (2021) Rockburst prediction and analysis of activity characteristics within surrounding rock based on microseismic monitoring and numerical simulation. *Int J Rock Mech Min Sci* 142:12. <https://doi.org/10.1016/j.ijrmmms.2021.104750>
- Xue YG, Li GK, Li ZQ, Wang P, Gong HM, Kong FM (2022) Intelligent prediction of rockburst based on Copula-MC oversampling architecture. *Bull Eng Geol Environ*. <https://doi.org/10.1007/s10064-022-02659-2>
- Yang BB, He MM, Zhang ZQ, Zhu JW, Chen YS (2022) A new criterion of strain rockburst in consideration of the plastic zone of tunnel surrounding rock. *Rock Mech Rock Eng* 55(3):1777–1789. <https://doi.org/10.1007/s00603-021-02725-3>
- Yang YL, Du LJ, Li QW, Zhao XB, Zhang WF, Liu ZY (2023) Predicting the accuracy and applicability of micro-seismic monitoring of rock burst in TBM tunneling using the data from two case studies in China. *Sustainability*. <https://doi.org/10.3390/su15054232>
- Yin X, Liu QS, Pan YC, Huang X (2021b) A novel tree-based algorithm for real-time prediction of rockburst risk using field microseismic monitoring. *Environ Earth Sci*. <https://doi.org/10.1007/s12665-021-09802-4>
- Yin X, Liu QS, Pan YC, Huang X, Wu J, Wang XY (2021c) Strength of stacking technique of ensemble learning in rockburst prediction with imbalanced data: comparison of eight single and ensemble models. *Nat Resour Res* 30(2):1795–1815. <https://doi.org/10.1007/s11053-020-09787-0>
- Yin X, Liu QS, Huang X, Pan YC (2021a) Real-time prediction of rockburst intensity using an integrated CNN-Adam-BO algorithm based on microseismic data and its engineering application. *Tunn Undergr Space Technol* 117. <https://doi.org/10.1016/j.tust.2021.104133>
- Yu SW, Ma JW, Wang WL (2019) Deep learning for denoising. *Geophysics* 84(6):V333–V350
- Yu Q, Zhao DC, Xia YJ, Jin SJ, Zheng J, Meng QK, Mu CQ, Zhao JC (2022) Multivariate early warning method for rockburst monitoring based on microseismic activity characteristics. *Front Earth Sci*. <https://doi.org/10.3389/feart.2022.837333>
- Zhai SB, Su GS, Yin SD, Yan SZ, Wang ZF, Yan LB (2020) Fracture evolution during rockburst under true-triaxial loading using acoustic emission monitoring. *Bull Eng Geol Environ* 79(9):4957–4974. <https://doi.org/10.1007/s10064-020-01858-z>

- Zhang M, Jiang FX (2020) Rock burst criteria and control based on an abutment-stress-transfer model in deep coal roadways. *Energy Sci Eng* 8(8):2966–2975. <https://doi.org/10.1002/ese3.715>
- Zhang GC, Gao Q, Du JQ, Li KK (2013) Rockburst criterion based on artificial neural networks and nonlinear regression. *J Cent South Univ* 44(7):2977–2981
- Zhang ZZ, Gao F, Shang XJ (2014) Rock burst proneness prediction by acoustic emission test during rock deformation. *J Cent South Univ* 21(1):373–380. <https://doi.org/10.1007/s11771-014-1950-3>
- Zhang R, Dai F, Gao MZ, Xu NW, Zhang CP (2015) Fractal analysis of acoustic emission during uniaxial and triaxial loading of rock. *Int J Rock Mech Min Sci* 79:241–249. <https://doi.org/10.1016/j.ijrmms.2015.08.020>
- Zhang CQ, Yu J, Chen J, Lu JJ, Zhou H (2016) Evaluation method for potential rockburst in underground engineering. *Rock Soil Mech* 37(Supp.1):341–349. <https://doi.org/10.16285/j.rsm.2016.S1.046>
- Zhang MW, Liu SD, Shimada H (2018) Regional hazard prediction of rock bursts using microseismic energy attenuation tomography in deep mining. *Nat Hazards* 93(3):1359–1378. <https://doi.org/10.1007/s11069-018-3355-3>
- Zhang JF, Li D, Wang YH (2020a) Predicting tunnel squeezing using a hybrid classifier ensemble with incomplete data. *Bull Eng Geol Environ* 79(6):3245–3256. <https://doi.org/10.1007/s10064-020-01747-5>
- Zhang JF, Wang YH, Sun YT, Li GC (2020b) Strength of ensemble learning in multiclass classification of rockburst intensity. *Int J Numer Anal Methods Geomech* 44(13):1833–1853. <https://doi.org/10.1002/nag.3111>
- Zhang LW, Zhang XY, Wu J, Zhao DK, Fu H (2020c) Rockburst prediction model based on comprehensive weight and extension methods and its engineering application. *Bull Eng Geol Environ* 79(9):4891–4903. <https://doi.org/10.1007/s10064-020-01861-4>
- Zhang SC, Ma TH, Tang CA, Jia P, Wang YC (2020d) Microseismic monitoring and experimental study on mechanism of delayed rockburst in deep-buried tunnels. *Rock Mech Rock Eng* 53(6):2771–2788. <https://doi.org/10.1007/s00603-020-02069-4>
- Zhang YH, Ma J, Sun DY, Zhang LY, Chen YC (2020e) AE characteristics of rockburst tendency for granite influenced by water under uniaxial loading. *Front Earth Sci*. <https://doi.org/10.3389/feart.2020.00055>
- Zhang C, Jin GH, Liu C, Li SG, Xue JH, Cheng RH, Wang XL, Zeng XZ (2021) Prediction of rockbursts in a typical island working face of a coal mine through microseismic monitoring technology. *Tunn Undergr Space Technol*. <https://doi.org/10.1016/j.tust.2021.103972>
- Zhang Q, Zheng T, Yuan L, Li X, Li W, Wang X (2024) A semi-Naïve Bayesian rock burst intensity prediction model based on average one-dependent estimator and incremental learning. *Tunn Undergr Space Technol*. <https://doi.org/10.1016/j.tust.2024.105666>
- Zhang J, Fu B, Li Z, Song S, Shang Y (2011) Criterion and classification for strain mode rockbursts based on five-factor comprehensive method, In: 12th ISRM Congress. OnePetro
- Zhao HB, Ru ZL, Yin S (2007) Updated support vector machine for seismic liquefaction evaluation based on the penetration tests. *Mar Geores Geotechnol* 25(3–4):209–220. <https://doi.org/10.1080/10641190701702303>
- Zhao GB, Wang DY, Gao B, Wang SJ (2017) Modifying rock burst criteria based on observations in a division tunnel. *Eng Geol* 216:153–160. <https://doi.org/10.1016/j.enggeo.2016.11.014>
- Zhao XG, Wang J, Cai M, Su GS (2021) Influence of intermediate principal stress on the strain-burst characteristics of beishan granite with consideration of end effect. *Rock Mech Rock Eng* 54(9):4771–4791. <https://doi.org/10.1007/s00603-021-02526-8>
- Zhou J, Li XB (2012) Integrating unascertained measurement and information entropy theory to assess blastability of rock mass. *J Cent South Univ* 19(7):1953–1960. <https://doi.org/10.1007/s11771-012-1231-y>
- Zhou J, Li XB, Shi XZ (2012) Long-term prediction model of rockburst in underground openings using heuristic algorithms and support vector machines. *Saf Sci* 50(4):629–644. <https://doi.org/10.1016/j.ssci.2011.08.065>
- Zhou J, Li XB, Mitri HS (2016) Classification of rockburst in underground projects: comparison of ten supervised learning methods. *J Comput Civ Eng*. [https://doi.org/10.1061/\(asce\)cp.1943-5487.0000553](https://doi.org/10.1061/(asce)cp.1943-5487.0000553)
- Zhou J, Li XB, Mitri HS (2018a) Evaluation method of rockburst: State-of-the-art literature review. *Tunn Undergr Space Technol* 81:632–659. <https://doi.org/10.1016/j.tust.2018.08.029>
- Zhou XP, Peng SL, Zhang JZ, Qian QH, Lu LC (2018b) Predictive acoustical behavior of rockburst phenomena in Gaoligongshan tunnel, Dulong river highway, China. *Eng Geol* 247:117–128. <https://doi.org/10.1016/j.enggeo.2018.10.023>

- Zhou ZL, Cheng RS, Chen LJ, Zhou J, Cai X (2019) An improved joint method for onset picking of acoustic emission signals with noise. *J Cent South Univ* 26(10):2878–2890. <https://doi.org/10.1007/s11771-019-4221-5>
- Zhou J, Koopialipoor M, Li EM, Armaghani DJ (2020) Prediction of rockburst risk in underground projects developing a neuro-bee intelligent system. *Bull Eng Geol Environ* 79(8):4265–4279. <https://doi.org/10.1007/s10064-020-01788-w>
- Zhou J, Guo HQ, Koopialipoor M, Armaghani DJ, Tahir MM (2021) Investigating the effective parameters on the risk levels of rockburst phenomena by developing a hybrid heuristic algorithm. *Eng Comput* 37(3):1679–1694. <https://doi.org/10.1007/s00366-019-00908-9>
- Zhou J, Yang PX, Peng P, Khandelwal M, Qiu YG (2023) Performance evaluation of rockburst prediction based on PSO-SVM, HHO-SVM, and MFO-SVM hybrid models. *Mining Metall Explor*. <https://doi.org/10.1007/s42461-022-00713-x>
- Zhu J, Deng JH (2023) Insights from a combined analysis of acoustic emission signals for water-bearing rocks in four-point bending tests: failure mode classification and strength degradation. *Rock Mech Rock Eng* 56(5):3843–3855. <https://doi.org/10.1007/s00603-023-03252-z>
- Zhu ZJ, Wu YL, Han J (2022) A prediction method of coal burst based on analytic hierarchy process and fuzzy comprehensive evaluation. *Front Earth Sci*. <https://doi.org/10.3389/feart.2021.834958>

Publisher's Note Springer Nature remains neutral with regard to jurisdictional claims in published maps and institutional affiliations.

Springer Nature or its licensor (e.g. a society or other partner) holds exclusive rights to this article under a publishing agreement with the author(s) or other rightsholder(s); author self-archiving of the accepted manuscript version of this article is solely governed by the terms of such publishing agreement and applicable law.